DOCTORA:
EDNA MARCELA RAMÍREZ OROZCO
DIRECTORA NUEVAS CREACIONES
SUPERINTENDENCIA DE INDUSTRIA Y COMERCIO
E. S. D.

REF. EXPEDIENTE No.:	**NC2018/0010549.**	
SOLICITUD PATENTE:	**COMPOSICIÓN ORALMENTE ADMINISTRABLE**	
SOLICITANTE:	**CTT PHARMA INC.**	

RESPUESTA A REQUERIMIENTO OFICIAL **OFICIO NO. 3504** NOTIFICADO EL 16 DE MARZO DE 2021.

CLAUDIA LUCIA CARO RAMIREZ, mayor de edad, domiciliada en Bogotá D.C., identificada con cedula No 40.017.374, en mi condición de apoderada de la sociedad **CTT PHARMA INC**, por el presente escrito y estando dentro del término legal para hacerlo, doy respuesta al oficio arriba referenciado, de acuerdo con lo siguiente:

En respuesta al oficio No. 3504, a continuación, encuentran:

i. Respuesta a los puntos del requerimiento
   - Respuesta punto por punto a los requerimientos del examinador.

ii. Adjunto a este memorial se presentan los siguientes documentos
   - Nuevo capítulo reivindicatorio.
   - Comprobante de pago por las modificaciones al capítulo reivindicatorio.
   - Extracto de los documentos citados en esta respuesta a requeirmiento de fondo
     - Smith et al. (Langmuir, 2009, 25 (19) 11239)
     - Liu et al. (Langmuir 2011, 27, 7926-7933)
     - Shrestha et al. (Advances in Colloid and Interface Science 279 (2020) 102162).

1. Título

El examinador objeta el titulo de la solicitud porque este no refleja el objeto y campo industrial de la solicitud de patente, el examinador recomienda modificar el titulo de la presente solicitud por:

UNA COMPOSICIÓN ADMINISTRABLE ORALMENTE QUE COMPRENDE UN AGENTE FORMADOR DE PELÍCULA FISIOLÓGICAMENTE ACEPTABLE COMBINADO CON UNA COMPOSICIÓN MICELAR QUE COMPRENDE UN CANNABINOIDE, EN NANO MICELAS ENCAPSULADAS, UN SOLVENTE ACUOSO FARMACÉUTICAMENTE ACEPTABLE Y UN EDETATO FARMACÉUTICAMENTE ACEPTABLE

El solicitante siguiendo las recomendaciones del examinador acepta la modificación propuesta y solicita que el título de la invención se modifique por el titulo propuesto por el examinador.

2. De la solicitud de patente.

Reivindicaciones

- El examinador objeta la reivindicación 5 porque esta hace referencia a las marcas comerciales "Phospholipon-H™ y "Phospholipon-G™", las cuales podrían cambiar sus composiciones en el tiempo y por tanto variar el objeto de la invención. El examinador sugiere definir los excipientes por los nombres genéricos o comunes

  El solicitante ha realizado las correcciones respectivas en la nueva reivindicación 4 (antigua reivindicación 5).

3. Determinación de Estado de la técnica:

Como resultado del examen de patentabilidad el examinador encontró los siguientes documentos relevantes:

Ítem	Documento	Título	Fecha de publicación
D1	WO2015068052	"Terpene and cannabinoid formulations"	14 de Mayo de 2015.
D3	WO2010002418	"Quick-Dissolving oral thin film for targeted delivery of therapeutic agents"	07 de Enero de 2010.

4. Examen de patentabilidad

Nivel inventivo

Inicia el examinador comparando las características técnicas de la reivindicación 4 de la solicitud colombiana NC2018/0010549 con la materia técnica revelada por D1 y D3, al finalizar dicha comparación, el examinador manifiesta que "*La diferencia entre la invención definida en la reivindicación 1 y lo revelado en el documento D1, consiste en el agente formador de película del 30 al 80 % en peso.*" (tomado del oficio 3504).

Asegura el examinador que:

> "*No se observa un efecto asociado a esta diferencia ya que a partir de la información de la descripción no es posible determinarlo. Luego de revisar el capítulo descriptivo y particularmente el ejemplo 1 (el único que se menciona en la descripción), no se observa ningún efecto técnico asociado a la formulación propuesta por el solicitante. Es más, no se observa que se solucione ningún problema técnico y que pueda comprobarse a partir de la información suministrada en el capítulo descriptivo, por tanto, el ejemplo 1*

simplemente corresponde a un procedimiento para la preparación de "obleas nanonizadas", pero esto no es suficiente para sustentar algún efecto técnico sorprendente o inesperado." (tomado del oficio 3504).

Por lo tanto, el examinador afirma que el problema técnico que se pretende resolver por la presente invención seria "*¿cómo modificar formulaciones micelares que comprenden un cannabinoide y un agente formador de película, reveladas en el documento D1, para proveer composiciones alternativas a las conocidas en el estado del arte?*" (tomado del oficio 3504).

Manifiesta el examinador que "*el documento D3 ya realizaba plenas sugerencias en el agente formador de película, para junto con las enseñanzas del documento D1, llegar a la presente invención. En el documento D3, se enseñan composiciones orales que contienen tiras de película fina de rápida disolución que comprenden agentes formadores de películas como el alginato en cantidades del 40 al 50%, la posibilidad de comprender un agente activo del tipo tetrahidrocanabinol y diferentes solventes*". (ejemplos I a IV; pág. 1, líneas 15 a 22; pág. 12, líneas 15 a 34; pág. 19, línea 1. D3)

De acuerdo con el anterior análisis el examinador concluye que una persona versada en la materia al observar los agentes formadores de películas en las cantidades señaladas del documento D3, habría podido adicionarlos en las formulaciones del documento D1, y así llegar al objeto de la reivindicación 1 de la solicitud. Por lo cual se considera obvia.

Continua el examinador manifestando que las reivindicaciones 2 a 12 tampoco cumplen con el requisito de nivel inventivo.

El solicitante quisiera manifestar su desacuerdo con el análisis del examinador.

El solicitante ha modificado la reivindicación 1 indicando que el agente formador de película comprende pululano y los compuestos formadores de micelas

comprenden un alquil sulfatos de metales alcalinos, un fosfolípido y glicerina. El soporte para esta modificación se encuentra descrito a lo largo del capítulo descriptivo, así como en el Ejemplo 1 que se encuentra en capitulo descriptivo y que abarca las páginas 17 a 20 del capítulo descriptivo tal y como se presentó el 1 de octubre de 2018. Se modifico el capítulo reivindicatorio de acuerdo con esta modificación y se eliminaron las antiguas reivindicaciones 2 y 7.

Para el solicitante es claro que los documentos citados tanto en el oficio 200538 como en el oficio 3504 (D1 a D3) no describen o sugieren de forma alguna la presente invención tal y como se reivindica en este nuevo pliego reivindicatorio, a continuación, amplio.

El documento WO2015/068052 (identificado acá como D1) enseña formulaciones de liposomas o micelas que comprenden uno o más terpenos y un cannabinoide en un solvente orgánico miscible en agua (por ejemplo, etanol) y opcionalmente, dichas formulaciones comprenden de forma adicional, un agente estabilizador como goma guar, alginato, gelatina, polivinilpirrolidona, celulosa, ácido hialurónico etc. Los ejemplos 1 y 2 (de D1) ejemplifican estas micelas. Es importante aclarar que las micelas que se obtienen en D1 son muy diferentes de las micelas reivindicadas en la presente invención (NC2018/0010549) las cuales se forman gracias a la inclusión de los tensioactivos particulares que aquí se reivindican; es decir, un alquil sulfatos de metales alcalinos, un fosfolípido y glicerina.

Por otro lado, el documento WO2010/002418 (identificado acá como D3) describe una composición de película fina de disolución rápida que comprende uno o más polímeros solubles en agua en los que se dispersa una o más micropartículas sensibles al pH que encapsulan un agente bioactivo. Las micropartículas comprenden un copolímero que es susceptible de degradación cuando se llega a un pH especifico, uno de los copolímeros descritos, corresponden a polímeros acrílicos o metacrílicos que se degradan en presencia de un pH básico. D3 también describe métodos para preparar la composición de película que comprende las micropartículas descritas anteriormente, dicho método se encuentra en las páginas

24 a 27. Como se muestra en D3, las micropartículas comprenden principalmente un agente bioactivo combinado con un polímero sensible al pH (Eudragit) en un solvente, que incluye opcionalmente una pequeña cantidad de Tween-20. Dichas micropartículas son muy diferentes de las micelas reivindicadas en la presente invención y que comprenden los agentes formadores de micelas específicos (un alquil sulfatos de metales alcalinos, un fosfolípido y glicerina).

Para el solicitante es claro entonces que los documentos citados (D1 y D3) No sugieren o enseñan una película que comprenda micelas formadas por un alquil sulfatos de metales alcalinos, un fosfolípido y glicerina que comprendan un cannabinoide. Por lo tanto, es claro que dichas micelas no habrían sido obvias a la luz de los documentos citados, ni por la combinación de los mismos. Esto último debido a que ni D1, ni D3 mencionan la mezcla de compuestos reivindicada para preparar micelas. De hecho, los documentos citados no se basan, revelan o incluyen el uso de tensioactivos para preparar sus micelas.

El solicitante también observa que la integración de nanopartículas tales como micelas en películas bucales mucoadhesivas es un desafío significativo ya que durante proceso de formación de películas generalmente da como resultado agregación de las nanopartículas lo que genera la incapacidad de retener el tamaño de partícula nanométrico deseado de las micelas. El solicitante proporciona, a continuación, varias referencias para confirmar que una persona versada en la materia tendría que haber sabido que la agregación de nanopartículas (que abarcan micelas) era un desafío significativo cuando se combinan nanopartículas en una película polimérica tal como pululano (como se reivindica en la presente solicitud).

- Smith et al. (Langmuir, 2009, 25 (19): 11239) este documento enseña que realizar una dispersión de nanopartículas en una matriz de polímero es intrínsecamente desafiante debido a las interacciones entrópicas desfavorables entre la matriz y las nanopartículas.

- Liu et al. (Langmuir 2011, 27, 7926-7933) enseña sobre la ocurrencia de agregación de nanopartículas en nanocompuestos poliméricos (ver abstract) lo que es un impedimento para el desarrollo de tales nanocompuestos (ver Introducción, primer párrafo). Liu et al. confirma que el termino nanopartículas se refiere tanto a nanopartículas orgánicas como inorgánicas.

- Shrestha et al. (Advances in Colloid and Interface Science 279 (2020) 102162) establece que:

  In all applications, the uncontrolled aggregation of NPs can have negative effects and needs to be avoided.

  "*En todas las aplicaciones, la agregación descontrolada de NPs* (nanopartículas) *puede tener efectos negativos y se debe evitarse* (ver Resumen, traducción libre).

Mientras que este documento si revela estrategias para minimizar la agregación, la estrategia que funcionaría en cada caso es muy particular, es decir, con las micelas y la matriz polimérica que se reivindica en la presente invención, no habría sido obvio para una persona versada en la materia, como se establece en la conclusión de este documento:

It is also apparent that the synthesis of NPs and keeping them in a nonagglomerated state or carrying out controlled aggregation for specific applications requires considerable chemical and physical insight;

(…)

There are numerous examples of real-world applications of NPs, and in each of these technologies, a thoughtful approach to avoid and/or control aggregation is important.

> *También es evidente que la síntesis de nanopartículas y mantenerlas en un estado no aglomerado o llevar a cabo una agregación controlada para aplicaciones específicas requiere un conocimiento químico y físico* ***considerable***; (traducción libre, subrayado fuera del texto original).
>
> (…)
>
> *Existen numerosos ejemplos de aplicaciones de nanopartículas en el mundo real, y en cada una de estas tecnologías, es importante un enfoque específico para evitar y/o controlar la agregación*. (traducción libre, subrayado fuera del texto original)

De acuerdo con lo anterior y en vista de los documentos citados anteriormente, una persona versada en la materia apreciaría claramente que la combinación de un polímero formador de película como el pululano con micelas sería un desafío, la persona versada en la materia entendería que la agregación de nanopartículas como las micelas es un impedimento para combinar dichos componentes, y se requiere un conocimiento considerable para evitar la agregación de las nanopartículas. Por lo tanto, para el solicitante es claro que la composición reivindicada no habría sido obvia para una persona versada en la materia, y que se requeriría una considerable experimentación para desarrollar una película que comprenda micelas que no se agreguen.

Así, se solicita al examinador que, en base a estos argumentos, reconsidere las objeciones relativas al nivel inventivo de la presente invención.

Por todo lo dicho, solicitamos que la Superintendencia de Industria y Comercio admita las modificaciones que se han facilitado, las cuales no amplían materia y subsanan las objeciones realizadas por el examinador. Asimismo, solicitamos que continúe el trámite con normalidad y se proceda con la concesión del Derecho sobre la Patente de la referencia.

Para efectos de notificaciones, recibiré estas vía internet al correo electrónico claudia.caro@ponsip.com, en la secretaría de esa Dirección y/o en la de la Delegatura de Propiedad Intelectual o en mi oficina de abogados de la Calle 94 A No 11A-32 Oficina 306 de la ciudad de Bogotá.

Agradezco su atención.

CLAUDIA LUCIA CARO RAMIREZ
CC No 40.017.374 de Tunja
T.P. No 36.448 del C.S de la J.
Adjunto lo anunciado.

Nuevo Capítulo reivindicatorio.

1. Una composición administrable oralmente que comprende al menos un agente formador de película fisiológicamente aceptable en una cantidad que varía del 30 al 80 % en peso combinado con una composición micelar, donde la composición micelar comprende un cannabinoide en una cantidad que varía del 0.1 al 30 % en peso de la composición encapsulada en nano micelas formadas mediante compuestos formadores de micelas cada uno en una cantidad que varía desde 1 a 10% en relación peso a peso de la composición total en un solvente acuoso farmacéuticamente aceptable, donde el agente formador de películas comprende pululano, y los compuestos formadores de micelas comprenden un alquil sulfatos de metales alcalinos, un fosfolípido y glicerina.

2. La composición de la reivindicación 1, en donde los compuestos formadores de micelas adicionalmente comprenden uno o más de los siguientes: alcoholes, ésteres o éteres de polioxietileno; ácidos biliares; lecitina, ácido hialurónico, sales farmacéuticamente aceptables de ácido hialurónico, octilfenoxipolietoxietanol, ácido glicólico, ácido láctico, ácido oleico, ácido linoleico, ácido linolénico, monooleína, monooleatos, monolauratos, aceite de borraja, aceite de onagro, extracto de manzanilla, extracto de pepino, mentol, trihidroxi oxo colanilglicina, lisina, polilisina, trioleína, polidocanol alquil éteres, polioxietilen 9-lauril éter, ácido cólico o una sal de este, ácido glicocólico o una sal de este, ácido quenodesoxicólico o una sal de este, ácido taurocólico o una sal de este, ácido glicodesoxicólico o una sal de este, ácido taurodesoxicólico o una sal de este, desoxicolato, esfingomielina y mezclas de estos.

3. La composición de la reivindicación 1, en donde los compuestos formadores de micelas comprenden un polioxietileno éter, un ácido biliar, una lecitina y mezclas de estos.

4. La composición de la reivindicación 1, en donde el alquil sulfatos de metales alcalinos es lauril sulfato de sodio y el fosfolípido se selecciona de lecitina

hidrogenada, fosfolípido saturado, lecitina enriquecida con fosfatidilcolina fosfolípido insaturado, fosfatidilcolina, fosfatidilserina, fosfatidiletanolamina, cefalina, lecitina, lisolecitina y mezclas de estos.

5. La composición de la reivindicación 1, en donde los compuestos formadores de micelas comprenden hialuronato sódico y lecitina hidrogenada, o lecitina enriquecida con fosfatidilcolina y ácido glicólico, o hialuronato sódico y lecitina.

6. La composición de la reivindicación 1, en donde el cannabinoide se selecciona del grupo que consiste en cannabidiol (CBD), ácido cannabidiol (CBDA), cannabinol (CBN), cannabigerol (CBG), ácido cannabigerol (CBGA), cannabidivarina (CBDV), ácido de cannabidivarina (CBDVA), cannabinovarina (CBNV), **c**annabigerovarina (CBGV) y cannabicromeno (CBC), delta-9 tetrahidrocannabinol (THC), delta-8 tetrahidrocannabinol (D8-THC), ácido tetrahidrocannabinol (THCA), tetrahidrocannabivarina (THCV), ácido tetrahidrocannabivarínico (THCVA) y mezclas de estos.

7. La composición de la reivindicación 1, en donde el agente formador de película adicionalmente comprende uno o más de metil celulosa, etil celulosa, carboximetil celulosa sódica, hidroxipropilmetil celulosa, hidroxietil celulosa, hidroxipropil celulosa, carboximetil celulosa, polivinil pirrolidona, polímeros de ácido metacrílico, copolímeros de ácido metacrílico, polímeros de ácido acrílico, copolímeros de ácido acrílico, poliacrilamidas, óxidos de polialquileno, carragenano, polivinil alcohol, alginato de sodio, polietilenglicol, ácido poliacrílico, glicolida, polilactida, copolímero de metilmetacrilato, carboxivinilo polímero, amilosa, almidón con alto contenido de amilosa, almidón con alto contenido en amilosa hidroxipropilado, ácido algínico, almidón de guisante, dextrina, pectina, quitina, quitosano, levan, elsinan y mezclas de estos.

8. La composición de la reivindicación 1, que comprende un agente formador de película secundario seleccionado del grupo que consiste en goma xantana, goma de tragacanto, goma de guar, goma de algarrobo, goma de acacia, goma

arábiga, colágeno, gelatina, zeína, gluten, aislado de proteínas de soja, aislado de proteínas de suero de leche, caseína y mezclas de estos.

9. La composición de la reivindicación 1, en donde el agente formador de película comprende una mezcla de pululano con uno o más agentes formadores de película seleccionados de alcohol polivinílico, carragenano, goma guar, goma xantana y goma de algarrobo.

10. La composición de la reivindicación 1, que comprende adicionalmente uno o más de: un agente plastificante, un agente saborizante, un agente precipitante de azufre, un agente estimulante de la saliva, un agente refrescante, un surfactante, un agente estabilizante, un agente emulsionante, un agente espesante, un agente aglutinante, un agente colorante, un edulcorante, y una fragancia.

SUPERINTENDENCIA DE INDUSTRIA Y COMERCIO

NIT: 800.176.089-2

COMPROBANTE DE RECAUDO SISTEMA SIPI

Radicado: NC2021/0007902
Recibo: 21-66294
Fecha: 16/06/2021

CLAUDIA LUCIA CARO RAMIREZ
CC: 40.017.374
Pago PSE No: 548347
CUS: 1026046305

NC Modificación a las reivindicaciones
Request on Patente PCT NC2018/0010549

Detalle del pago

Id.	Rentístico	Concepto y Servicio	Cant.	Val. Unit.	Subtotal
1	50005-01-03	Modificaciones / Correcciones al registro Patente PCT (DESCUENTO INTERNET)	1	$ 171,500	$ 171,500
		TOTAL			$ 171,500

Sede Centro: Carrera 13 No.27-00 Pisos 3,4,5 y 10 Bogotá D.C. - Colombia
Web: www.sic.gov.co e-mail:contactenos@sic.gov.co Conmutador:(571)5870000 Contact Center: (571)5920400

Langmuir. 2009 Oct 6;25(19):11239-43. doi: 10.1021/la902329v.

Dispersing nanoparticles in a polymer matrix: are long, dense polymer tethers really necessary?

Grant D Smith [1], Dmitry Bedrov

Affiliations
PMID: 19788206 DOI: 10.1021/la902329v

Abstract

Dispersing nanoparticles in a polymer matrix is intrinsically challenging because of unfavorable entropic interactions between the matrix and the nanoparticle. Similar to suspensions of larger colloidal particles, it has been found that thermodynamically stable dispersions of nanoparticles can be achieved in polymer matrices when the nanoparticles are decorated with dense layers of polymer tethers whose molecular weight is comparable to or greater than that of the matrix. Utilizing molecular dynamics simulations, we demonstrate that, in contrast to larger colloidal particles, repulsive interactions between nanoparticles can be achieved with tethered polymers much shorter than the polymer matrix when relatively sparse grafting is employed.

LinkOut - more resources

Full Text Sources
American Chemical Society

Langmuir ARTICLE

pubs.acs.org/Langmuir

Nanoparticle Dispersion and Aggregation in Polymer Nanocomposites: Insights from Molecular Dynamics Simulation

Jun Liu,[†,‡] Yangyang Gao,[†] Dapeng Cao,[*,†,‡] Liqun Zhang,[*,†] and Zhanhu Guo[*,§]

[†]Key Laboratory of Beijing City on Preparation and Processing of Novel Polymer Materials and [‡]Division of Molecular and Materials Simulation, State Key Laboratory of Organic–Inorganic Composites, Beijing University of Chemical Technology, Beijing 100029, People's Republic of China

[§]Integrated Composites Laboratory (ICL), Dan F. Smith Department of Chemical Engineering, Lamar University, Beaumont, Texas 77710, United States

ABSTRACT: It is a great challenge to fully understand the microscopic dispersion and aggregation of nanoparticles (NPs) in polymer nanocomposites (PNCs) through experimental techniques. Here, coarse-grained molecular dynamics is adopted to study the dispersion and aggregation mechanisms of spherical NPs in polymer melts. By tuning the polymer–filler interaction in a wide range at both low and high filler loadings, we qualitatively sketch the phase behavior of the PNCs and structural spatial organization of the fillers mediated by the polymers, which emphasize that a homogeneous filler dispersion exists just at the intermediate interfacial interaction, in contrast with traditional viewpoints. The conclusion is in good agreement with the theoretically predicted results from Schweizer et al. Besides, to mimick the experimental coarsening process of NPs in polymer matrixes (*ACS Nano* 2008, *2*, 1305), by grafting polymer chains on the filler surface, we obtain a good filler dispersion with a large interparticle distance. Considering the PNC system without the presence of chemical bonding between the NPs and the grafted polymer chains, the resulting good dispersion state is further used to investigate the effects of the temperature, polymer–filler interaction, and filler size on the filler aggregation process. It is found that the coarsening or aggregation process of the NPs is sensitive to the temperature, and the aggregation extent reaches the minimum in the case of moderate polymer–filler interaction, because in this case a good dispersion is obtained. That is to say, once the filler achieves a good dispersion in a polymer matrix, the properties of the PNCs will be improved significantly, because the coarsening process of the NPs will be delayed and the aging of the PNCs will be slowed.

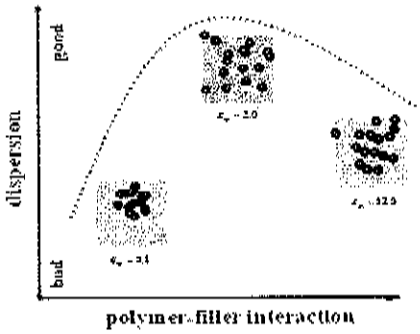

1. INTRODUCTION

Polymer nanocomposites (PNCs), by dispersing organic or inorganic nanoparticles (NPs) such as spheres, rods, and plates in polymer matrixes, have attracted considerable academic and industrial attention. PNCs always possess greatly enhanced mechanical, optical, electrical, and flame retardancy properties and so on.[1] However, one main impediment in the development of high-performance PNCs is to realize a good dispersion of NPs, owing to the strong interparticle interactions and weak polymer–nanoparticle interfacial interaction. To address this issue, various experimental, theoretical, and simulation studies have been performed. For instance, Mackay et al.[2,3] found that a thermodynamically stable dispersion of NPs in a polymer matrix can be enhanced only when the radius of gyration of the linear polymer chain is greater than the radius of the nanoparticle, however, which can be obtained only with the correct processing strategy. Similarly, in the case of cross-linked polystyrene (PS) NPs mixed with linear PS chains, the key role of entropy in the nanoparticle dispersion is indentified.[4] Meanwhile, Krishnamoorti[5] has reviewed various experimental methods to quantitatively characterize the nanoparticle dispersion, such as atomic force microscopy (AFM), transmission electron microscopy (TEM), and scattering, electrical, and mechanical spectroscopy. By considering the qualitative TEM images as the "gold standard" for dispersion characterization, Khare et al.[6] have also developed a free-space length method to quantitatively analyze the dispersion of NPs.

Recently, by using the microscopic polymer reference interaction site model (PRISM), Schweizer et al.[7] found that, for hard-sphere fillers, four general categories of polymer-mediated nanoparticle organization exist: (i) contact aggregation, (ii) segmental-level tight particle bridging, (iii) steric stabilization due to thermodynamically stable "bound polymer layers", and (iv) "tele-bridging". Furthermore, they also obtained three dispersion phase diagrams for hard fillers: (i) macroscopic phase separation at low polymer–filler interaction, (ii) enthalpically stabilized miscible fluid at moderate interfacial interaction, and (iii) microscopic phase separation through local bridging of the fillers by polymer chains. Very recently, Ganesan et al.[8] reviewed advances of the equilibrium dispersion and structure of PNCs on the basis of

Received: March 22, 2011
Revised: May 6, 2011
Published: May 19, 2011

Advances in Colloid and Interface Science 279 (2020) 102162

Contents lists available at ScienceDirect

Advances in Colloid and Interface Science

journal homepage: www.elsevier.com/locate/cis

Historical perspective

Nanoparticle processing: Understanding and controlling aggregation

Sweta Shrestha [a], Bo Wang [a], Prabir Dutta [b,*]

[a] ZeoVation, 1275 Kinnear Road, Columbus, OH 43212, United States of America
[b] Department of Chemistry and Biochemistry, The Ohio State University, Columbus, OH 43210, United States of America

ARTICLE INFO

Article history:
13 April 2020
Available online 16 April 2020

Keywords:
Synthesis
Stabilization
Surface charge
Drying
Agglomeration

ABSTRACT

Nanoparticles (NPs) are commonly defined as particles with size <100 nm and are currently of considerable technological and academic interest, since they are often the starting materials for nanotechnology. Novel properties develop as a bulk material is reduced to nanodimensions and is reflected in new chemistry, physics and biology. With reduction in size, a greater function of the atoms is at the surface, and promote different interaction with its environment, as compared to the bulk material. In addition, the reduction in size alters the electronic structure of the material, resulting in novel quantum effects. Size also influences mobility, primarily controlled by Brownian motion for NPs, and relevant in biological and environmental processes. However, the small size also leads to high surface energy, and NPs tend to aggregate, thereby lowering the surface energy. In all applications, the uncontrolled aggregation of NPs can have negative effects and needs to be avoided. There are however examples of controlled aggregation of NPs which give rise to novel effects. This review article is focused on the NP features that influences aggregation. Common strategies for synthesis of NPs from the gas and liquid phases are discussed with emphasis on aggregation during and after synthesis. The theory involving Van der Waals attractive force and electrical repulsive force as the controlling features of the stability of NPs is discussed, followed by examples of how repulsive and attractive forces can be manipulated experimentally to control NP aggregation. In some applications, NPs prepared by liquid methods need to be isolated for further applications. The process of solvent removal introduces new forces such as capillary forces that promote aggregation, in many cases, irreversibly. Strategies for controlling aggregation upon drying are discussed. There are also many methods for redispersing aggregated NPs, which involve mechanical forces, as well as manipulating capillary forces and surface characteristics. We conclude this review with a discussion of aggregation relevant real-world applications of NPs. This review should be relevant for scientists and technologists interested in NPs, since emphasis has been on the practical aspects of NP-based technology, and especially, strategies relevant to controlling NP aggregation.

Contents

* Corresponding author.
E-mail address: dutta.1@osu.edu (P. Dutta).

https://doi.org/10.1016/j.cis.2020.102162
0001-8686/

1. Nanoparticles: practical relevance of aggregation

1.1. Definition of nanoparticles

Materials formed with nanometer dimensions have properties quite distinct from their bulk counterparts or the discrete ions that make up the material. These properties are manifested in novel reactivity, electrical, mechanical and magnetic properties. Extensive interest in this topic is evident from the large number of publications and patents, and these cited references are a sampling from the numerous books and manuscripts [1–8].

Nanoparticles (NPs) are defined as a material with at least one of its dimensions in the size range of 1–100 nm, and can appear as nanoparticles, nanotubes, nanofilms and bulk nanomaterials such as dendritic structures. Another proposed definition is that nanomaterials exhibit a specific surface area to volume ratio greater or equal to 60 m^2/cm^3 [9]. In this review, we primarily deal with nanoparticles. In the nanosize range, a large fraction of the atoms making up the NP are at the surface. For example, palladium NPs of radii 1, 2, 10 and 50 nm will have 62, 38, 8 and 2% of the total atoms on the surface of the particle.

1.2. Aggregation

NPs as synthesized, tend to be very reactive since their surfaces possess a high density of dangling bonds, and defects. Due to the small grain sizes, the surface energy is high, and processes to reduce the surface energy through assembling of NPs can become dominant [10]. Agglomerates are defined as weakly bound collection of NPs, whereas, aggregates are tightly bound collection of NP, the latter being difficult to break up into primary particles by mechanical forces.

Uncontrolled aggregation adversely influences the functionality of NPs. In a media, the surface energy can decrease by dissolution into smaller species, or aggregation [1]. In order to use and benefit from the attractive features of NPs, both these processes need to be arrested. Dissolution and particle growth of the remnant particles can proceed in the reaction medium and is referred to as Ostwald ripening. Aggregation can be thwarted by coating the NP via surface engineering with charged groups or by steric means. In that case, a NP is to be understood as a single entity comprising both the material and surface groups. Strategies that exploit the application of NPs require that the NPs be dispersed within the medium of interest without aggregation. The size of the NPs as well as its loading will determine the strategies to minimize aggregation.

Change of property on aggregation is manifested in many ways, including reactivity, photoreactivity, surface area, bioavailability and toxicity. Reactivity is altered since less surface is exposed and is relevant for catalysis. In environmental applications, such as pollutant remediation by zero-valent iron particles, aggregation influences mobility, thereby sacrificing the ability to get to the pollutant, as well as decreasing the reactivity. Reactivity is also influenced by particle size, e.g., with decreasing size of ZnO and TiO_2 aggregates, hydroxyl radical formation increased [11]. Another example of reactivity is dechlorination of carbon tetrachloride, where the rate decreased as 9 nm magnetite particles aggregated [12]. Attempts at stabilizing the surface reactive sites, e.g., by means of ligand attachment can provide non-aggregated nanoparticle dispersions [13].

Interestingly, controlled aggregation of NP is beneficial for certain applications, e.g., aggregation into three-dimensional structures is relevant for photonic, surface-enhanced Raman and magnetic applications. Controlled aggregation is possible by a two-step process, the first involving formation of well dispersed NPs, and then triggering a controlled assembly via some external perturbation. This external force can be controlled drying, electrical, optical, magnetic or chemical perturbation via ligand or solvent modification [3].

2. Influence of synthesis on aggregation

The synthesis method for a particular NP can have a profound influence on the aggregation characteristics. NPs are typically synthesized in either the gas phase or liquid phase.

2.1. Gas phase

Fig. 1 shows the relevant processes for particle formation in the gas phase. Briefly, precursors have to be generated in the gas phase, which

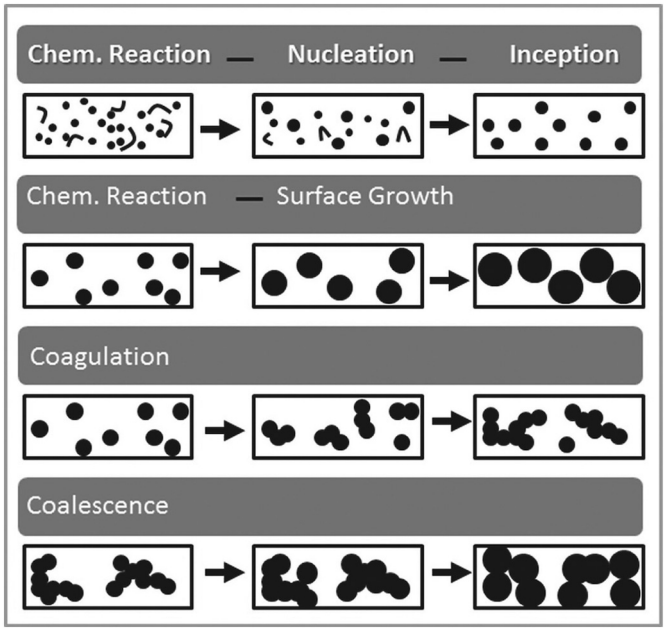

Fig. 1. Depiction of the various steps occurring in gas-phase synthesis of particles. (taken from Reference [14]).

decompose to form supersaturated states, leading to nucleation. The next steps involve surface growth to form the primary NPs, along with unwanted effects of coagulation and coalescence. Coagulation results from joining of particles via collisions, and coalescence is the fusion on particles. NPs prepared by gas-phase methods are prone to agglomeration promoted by collision of particles, as well as particle growth by interparticle sintering at elevated temperatures. Nevertheless, there is considerable commercial driving force for gas phase synthesis, because these processes tend to be rapid, and scalable to large quantities (1000 g/h) [14,15].

The eventual state of aggregation in gas phase synthesis methods is dependent on the time-temperature profile during and after particle growth [16]. It has been shown for silica particles that the cooling rate determines whether the primary particles are loosely agglomerated or sintered [17]. For flames and microwave plasmas, high cooling rate suppress sintering, whereas in hot-wall reactors, because of the lower heating and cooling rates, large sintered aggregates are formed. Plasma synthesis results in non-aggregated spherical particles, where size can be adjusted by pressure and precursor concentration. Lower operating pressures and lower concentration can minimize aggregation, but at the expense of yield. Repulsive Coulomb interactions keeps charged particles separated.

Flame spray pyrolysis involves evaporation of metal chlorides into flames to produce oxides, examples being zirconia and silica. Hot wall reactors and laser pyrolysis are other gas phase methods that are typically practiced on a laboratory scale to make nanoparticles, except for Al-doped TiO_2, which is done on a large scale in a hot wall reactor [18].

Flame spray synthesis can make a wide range of materials, including TiO_2, CeO_2, Bi_2O_3, metal oxides with precious metal catalysts, Pt/TiO_2, Pd/CeO_2, ternary mixed metal oxides, $Ce_xZr_yO_z$, indium tin oxide, spinels, perovskites, fluorapatites and calcium phosphates. [16,19–21].

Plasma and chemical vapor deposition are methods to generate nanoparticles onto surfaces of substrates. Particle nucleation and growth proceeds from a highly supersaturated state formed via thermal decomposition of precursors. Precursors are typically metal organics or metal salts.

Mechanical grinding of aggregated particles is often practiced to make nanoparticles, but the particle size is typically broad and impurities can get incorporated from wearing of the milling agent [22].

Chemically-bonded agglomerates are attractive for certain applications, e.g., catalysis, fiber optics and electroceramics (e.g. battery). By controlling the high temperature particle residence time in flames, fractal-like nanoaggregate structures can be formed [23].

2.2. Liquid phase

To make well-dispersed NPs in the liquid phase, one can exploit the chemistry, viscosity of the liquid, as well as addition of surface-active compounds [14]. Liquid-based methods can avoid agglomeration via surface functionalization and manipulation of surface charge. The strategy is to exploit the balance between attractive Van der Waals, electrostatic repulsion, hydrogen bonding, steric effects, and hydrophobic interactions to promote NP dispersion.

The formation of NPs in the liquid phase typically proceeds from soluble precursors, which go on to form a sparingly soluble species in a supersaturated state resulting in nucleation. The growth of the nuclei into NP requires that the free energy of the growth process can compensate for the formation of the new interface. In this classical model, the transformation of nuclei to NP is rapid, thus concentration of nuclei in the solution is not significant. Recent work is showing that this process can be more complicated, with the existence of liquid-like prenucleation clusters, which can aggregate to form amorphous clusters and evolve into crystals, as observed for $CaCO_3$ and $CaSO_4$ [24].

Aggregation limited only by the diffusion of the NP to the growing cluster, leads to highly disordered clusters [3,25]. Another strategy to make isolated NPs is to use confinement, for example, using the water pocket of reverse micelles or cages of zeolites for NP growth [26,27]. It is difficult to make large quantities of NPs by these confinement methods, and isolation of the particles is difficult.

Precipitation to purify NP and resuspension can lead to aggregation of NP. Centrifugation is a common method to isolate NP, but the disadvantage is that it is a batch process and can be limited in capacity. Filtration is another route to separate NP for purification, but requires filters with nanofiber networks, and is prone to fouling and clogging of the nanopores.

Device fabrication can promote an inherent heterogeneity in the particle distribution. Integration into devices will require proper spatial control of NPs. Inkjet printing is a technology for fabrication of devices from NPs. Electric fields and electrospinning find use for fabrication with NPs. Simpler process for NP synthesis/fabrication appears to be more robust. NPs stabilized by steric exclusion are more robust to changes in ionic strength, as compared to electrostatic stabilization.

3. Stabilization of NP towards aggregation

3.1. Theory

There are different forces that can act on NP in a liquid medium, and determine its stability, as shown in Table 1 [3,28]. When two particles collide, either they attach or they repel. The primary attractive force is Van der Waals (VDW). It is proportional to particle size, has a power law dependence on interparticle distance and extends to longer distances. VDW is inversely proportional to square of particle separation and can have extremely deep minima as particles come closer. The basis of this attractive force is fluctuating electromagnetic fields (fluctuating dipoles) generated via polarization effects. This is dependent on the refractive index and optical properties (mainly UV relaxation) of the intervening medium, and captured by the Hamaker constant (A_H, typical values of $0.3–10 \times 10^{-20}$ J). However, if the particles get too close to each other and result in orbital overlap, it will lead to repulsion (Born repulsion). The entire effect can be represented by a Lennard-Jones potential.

The repulsive forces arise from the electrical double layer (EDL) around the particles. The EDL arises from the charged surface and counterions around it. The charge can also develop due to the surface OH groups (on deprotonation the charge is negative, on protonation, the charge is positive). As the particles approach, and the EDL begins to overlap, and there is repulsion. A measure of the electrical potential and its charge can be estimated from zeta potential (ZP). ZP is the charge at the shear plane (Stern plane), and not the charge on the particle surface. EDL scales as square of ZP and decreases exponentially with distance from the particle surface. The fall off is given by the Debye-Huckel parameter and its inverse is a measure of the thickness of the diffuse layer that moves with the particle. The diffuse layer

Table 1
Forces influencing the stability of NPs in liquid medium.
(adapted from Reference [10]).

Force	Influence
Van der Waals	Short range electromagnetic force between NPs, attractive in nature
Electrical double layer	Electrical interaction between NP due to the overlap of electric double layer, typically repulsive
Hydration force	Interaction between water molecules on hydrophilic NPs, repulsive in nature
Hydrophobic force	Attractive interaction between hydrophobic NPs in water
Steric, electronic and electrostatic forces	Surface coatings; Inorganic, Surfactants, polymers and polyelectrolyte on NP surfaces. Polymers can form bridges leading to osmotic forces for interpenetrates chains. Surface coatings can have attractive or repulsive effects.

thickness decreases with increasing ionic strength and decreases the repulsive force. At point of zero charge (PZC), the surface is neutral. Isoelectric point (IEP) is where ZP is zero, and PZC can be different from IEP. PZC is influenced by particle size, since the number and coordination of surface atoms vary with size, e.g. 12, 32 and 65 nm hematite particles had PZCs of 7.8, 8.2 and 8.8 pH units, respectively, suggesting that at neutral pH, the smaller particles are less charged and will aggregate more [29]. Crystal structure can also influence ZP, e.g. for anatase TiO_2, the ZP is −20 mV, whereas for rutile polymorph of TiO_2 it is −35 mV [30].

DLVO theory combines VDW attractive force and EDL repulsive force to predict the overall force between particles. Van der Waals forces fall off as the inverse of the square of the interparticle distance, whereas electrical repulsive forces fall of exponentially. Thus, as particles approach, the repulsive force poses a barrier. The heights of the energy barrier determine if collision energy can exceed it and promote aggregation. Typically, a barrier is kinetically stable if the barrier energy exceeds 10kT [31].

An attachment efficiency can be defined (α_a) as the probability that a collision results in two particles bonding. Stability ratio ω is defined as $1/\alpha_a$. Critical coagulation concentration (CCC) is the concentration of ions that make $\omega = 0$, indicating no energy barrier. CCC is inversely dependent on charge (z^{-6}) of the added ions and is smaller as charge of ions increases. Higher ionic strength and increased valence of counterions decreases the interparticle repulsive force [32]. Thus, CCC of C_{60} NP is 4.8 mM for Ca^{2+} and 120 mM for Na^{+}, demonstrating that divalent ions will promote NP aggregation [33].

Larger values of A_H promote aggregation, whereas increased surface potential leads to repulsion As an example, the A_H for Fe_2O_3 is 8.2×10^{-18} J, and for *E. coli* 7.0×10^{-19} J, leading to a 12 times stronger VDW attraction for the Fe_2O_3 particles [34]. Another example is gold and polystyrene with Hamaker constants of 45.3×10^{-20} and 9.8×10^{-20} J, respectively, leading to a fivefold stronger attraction for gold [35].

Aggregation rate of particles is described by.

$$dn/dt = k_a n^2 \quad (1)$$

$$k_a = \alpha_a \beta \quad (2)$$

$$k_a = 4k_bT/3\lambda \text{ (for } \alpha_a = 1) \quad (3)$$

where n is the number concentration of particles, k_a is the second-order rate constant, β is the mass transport coefficient and α_a is the attachment efficiency ($\alpha_a = 1$ if there is no energy barrier and determines the maximum aggregation rate otherwise $\alpha_a < 1$), k_b is the Boltzmann constant, T the temperature, and λ the dynamic viscosity. Stability ratio ω is.

$$\omega = 1/\alpha_a = 2\, k\, a_p \ \exp.(-V_{max}/k_bT) \quad (4)$$

where V_{max} is the barrier height, k is the inverse Debye length, and a_p is the particle radius [36,37].

DLVO theory predicts that the height of the energy barrier and the depth of secondary minimum will increase with particle size [32]. Electrostatic stabilization of NP will be different depending on the polarity of the solvent, the theoretical underpinnings are better developed for aqueous systems [31]. NPs with ZP ranging from −30 to −40 mV (or comparable positive values) are considered stable, and with further negative ZP, the NPs are more stabilized [38,39].

An example shown in Fig. 2 will assist in understanding the implications of DLVO theory [10]. For a 20 nm particle with surface charge of 64.9 mV in a solution with counter-ion concentration of 0.6 mM (corresponding to a thickness of ~12.4 nm for the electrical double layer), the peak value of the potential curve is 3kT. Under similar conditions, for a 300 nm particle, the peak value of the potential curve is 35 kT. If the peak value of the potential curve is <10–20 kT, then the particle will aggregate, implying that the ~20 nm suspension will aggregate, whereas the ~300 nm suspension will not. For the ~20 nm suspension to be stable (~35 kT peak of potential), the surface potential will have to be ~177 mV with counter ion concentration of 1 mM. Such a high surface charge is difficult to obtain by adsorption of ions [10]. NP aggregation tends to follow a fractal pattern [34]. With low attachment frequency, aggregates are more compact, whereas with higher attachment frequency, dendritic aggregates are formed [40,41].

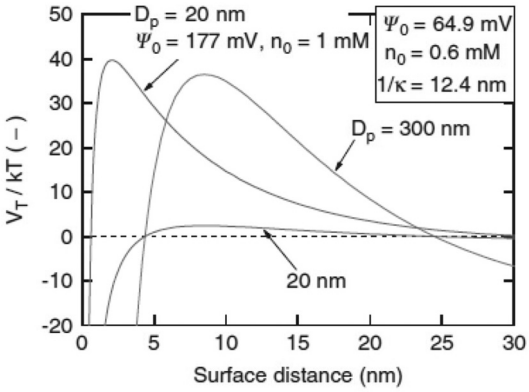

Fig. 2. Calculated potential curves based on DLVO theory, showing dependence on particle diameter and surface charge.
(taken from Reference [10]).

3.1.1. Non-DLVO forces

There can be non-DLVO forces that influence aggregation [42]. These include hydration forces, where H_2O layers interact; and hydrophobic forces controlled by entropic factors related to water ordering. Osmotic forces also arise due to entropic changes, as in NPs with polymer coatings interacting with each other via interpenetrating chains. NP surface coatings with surfactants, polymers and polyelectrolytes manifest interparticle repulsion via steric, electronic and electrostatic effects [31,43]. Increase in temperature of a suspension of NP results in increased Brownian motion and decrease in water shear, promoting aggregation [34]. However, for forming a suspension with particles compatible with the solvent, temperature increase can promote motion and thereby the dispersion.

Hydration forces are manifested when particle separations are ~1 nm, and are repulsive, due to energy required to remove the water layer hydrating the charge surfaces [32]. Particles with hydrophobic surface will feel an attractive force as structured water is released to bulk-like water. Hydrophobic forces between surfaces are attractive and exist over both short (1–2 nm) and longer (100 nm) distances [32]. Hydrophobic particles will aggregate in water, thereby minimizing the particle interface [32].

Steric interactions, typically arising from polymeric coatings on the surface are repulsive, since the polymers "pack" between particles and reduce entropy. However, if the polymer chains can form bridges between particles, that would result in an attractive force [32]. Hydrophilic polymers will favor repulsion since energy is required to remove hydrated water. Weak polymer held aggregates can be broken by shear. A form of "reactive" aggregation has been noted for AgNP in the presence of sulfide ions. The AgS formed on the surface of AgNP acts as a bridge between the NP [44].

3.2. Liquid phase stabilization

Many strategies have been developed to make stable NP suspensions, and we discuss these in the present section. Physical/mechanical forces are not very effective for NP dispersion. Particle dispersibility is

more effective if insitu surface modifications are carried out during synthesis, rather than by post-synthesis modifications [10].

3.2.1. NP concentration

The concentration of particles determines interparticle distance, and is an important parameter to determine stability. As seen in Fig. 2, the maximum repulsive potential appears at distances of several nanometers between the surfaces (e.g. for 300 nm particles, it is ~8–10 nm). It is possible to calculate the mean surface distance h_{susp} between the particles as a function of NP solid loading using Woodcock's equation [10]:

$$h_{susp} = D_p \left[\{1/(3\pi F) + 5/6\}^{0.5}\right] \quad (5)$$

where F is the solid fraction and D_p is the particle diameter.

Fig. 3 shows the surface distance as a function of solid loading for the 300 and 20 nm particles [10]. If the concentration of the 300 nm dispersion were to exceed 40 vol%, the mean surface distance between NP is ~10 nm, then surface repulsive forces (electrical double layer) alone will not be sufficient to keep particles from aggregating. However, at 10 vol%, the interparticle distance significantly exceeds 10 nm, and stable dispersion using DLVO type interaction is possible. To make up dispersions with the higher loadings (>40 vol%), additional steric repulsive forces, such as those possible with surface modification is required. For the 20 nm particles, loadings will need to be lowered further (<5 vol%) to stabilize the suspension using the DLVO forces.

A practical upper limit for stable metal dispersion is also mentioned in the literature. For example, with 10 nm citrate-covered AuNP, a stable dispersion concentration is 10^{16} NP/ml corresponding to 10 μM, with average interparticle distance of 100 nm, and mass concentration of a few mg/ml [1].

3.2.2. Surface charge

Surface modifications influence NP aggregation via non-DLVO interactions, including steric, hydrophobic, magnetic and hydration effects. Manipulation of surface potential influences aggregation, values lower than 20 mV can cause aggregation [10]. Altering pH and ionic strength can influence aggregation in aqueous systems. The effect of pH is closely linked to PZC. For example, iron oxide with a PZC at pH 9.1 shows a slight increase in size from pH 2 to 6, followed by a rapid increase at pH > 6, maximizing around pH 8.5, indicating increased aggregation at pH close to PZC [45]. The optimum pH for aqueous dispersion of alumina, copper (with surfactant SDBS) and graphite are 8, 9.5 and 2, respectively [46,47]. Another example is fullerol aggregates growing in size as pH shifts towards PZC [48].

Increase in ionic strength decreases the electrical double layer, allowing for closer approach of particles, and enhancing aggregation. Ions can also adsorb on the NP surface, altering the sign and magnitude of zeta potential. For example, 50–60 nm TiO_2 increased to micron size with increase of ionic strength, from 4.5 to 16.5 mM NaCl solution. Divalent ions have a stronger effect on aggregation, as compared to monovalent ions as evidenced with citrate and π-mercaptoundecanoic acid covered AuNP, with aggregation following $Ca^{2+} = Mg^{2+} >> Na^{+}$ because of increased suppression of the electrical double layer [49]. The coarsening of ZnO NPs (<10 nm) synthesized from the acetate, bromide and perchlorate salts followed the order $Br^{-} < COOCH_3^{-} < ClO_4^{-}$, indicating that the rate of aggregation is dependent on adsorption of anions on the NP surface [50].

3.2.3. Surface coatings

Surface coatings on NP can include covalent methods such as silica coating, as well as polymer, surfactant coatings that function via electrostatic interactions [2]. An example shown in Fig. 4, where a silica coating on hydrophilic Fe_2O_3 NP introduced by hydrolysis of TEOS with ammonia led to particles that can be dispersed in water or ethanol [2,51,52].

With titania, coatings of silica, alumina and aluminosilicate lead to stable suspensions. In one such example, titania was coated with an aluminosilicate layer by adding silicic acid and aluminate solution. The aluminosilicate shell has a high negative charge and stabilizes the titania suspension between pH 3 to 7. Aluminum doping decreases the aggregation of TiO_2 crystals upon calcination, and proposed to result from lower surface energy [53]. Alumina coatings on TiO_2 prepared by mixing alumina powder with metatitanic acid, followed by calcination resulted in better dispersion, and it was proposed that alumina with its lower Hamaker constant decreased the VDW attractive force [54].

Polymer coatings are also used widely. In case of nonionic polymer coatings, steric effects can keep particles apart (Fig. 5a), but the molecular weight of the polymer is relevant, since tangling of polymer chains in different particles can cause aggregation (Fig. 5b). Ionic polymer coatings manifest their effect via electrostatic forces, and with anionic polymers, a method to manipulate the interparticle force is through choice of cations (e.g. K^{+} vs Ba^{2+}). Examples of polymer dispersants include nonionic polymer dispersants such as poly(vinylpyrrolidone), anionic polymers such as polycarboxylic acid, and cationic polymers such as polyethyleneimine [55–57]. Water dispersion for hydrophobic particles can be achieved with polymers with both hydrophilic and hydrophobic groups, e.g. $BaTiO_3$ aqueous dispersions can be made with polymers that have poly(acrylic) acid and poly (ethylene oxide) units [58].

More complicated chemistry is also possible with polymer coatings. By adsorbing anionic poly(styrene sulfonate) (PSS) on positively charged layered double hydroxides (Mg, Al), the composite gradually reaches IEP, is precipitated out, and with further PSS, the composite becomes negatively charged and can be dispersed. Further adsorption of

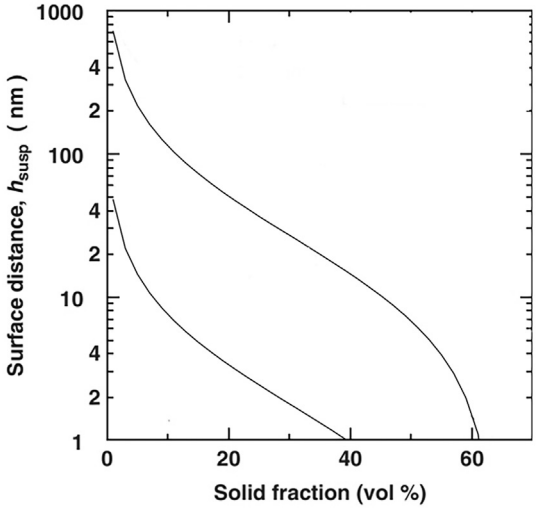

Fig. 3. Dependence of the mean surface distance between particles for sizes of 20 and 300 nm with varying solid fraction (vol%) of the particles.
(adapted from Reference [10]).

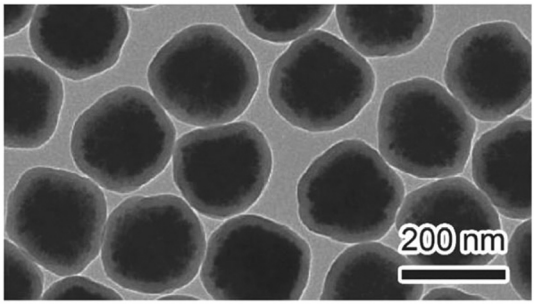

Fig. 4. TEM image of Fe_2O_3 NPs coated with silica.
(taken from Reference [2]).

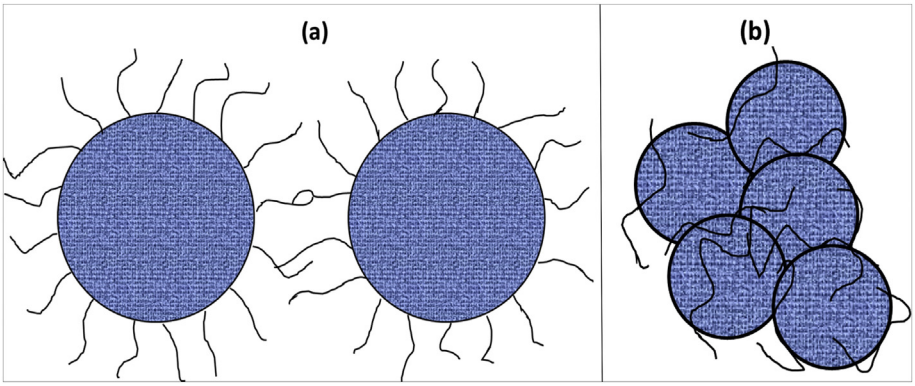

Fig. 5. (a) Two particles avoiding contact due to surface bound polymer chains (b) Bridging of polymer chains leading to aggregation. (adapted from Reference [42]).

cationic poly(diallyldimethyl ammonium chloride) (PDADMAC) on the PSS-LDH can render the composite charge positive again, with the hydrodynamic ratio increasing from 167 to 216 and finally 352 nm for LDH, PSS-LDH and PDADMAC-PSS-LDH, respectively. From a practical point of view, the propensity for salt induced aggregation reduced with the PSS-LDH (1000 mM NaCl) as compared to LDH (50 mM NaCl) due to repulsive steric interactions between the polymer chains on the PSS-LDH sample [59]. Similar strategies also worked with halloysite nanotubes using protamine sulfate polyelctrolytes [60] and titania nanosheets using PSS, and provided protection against salt induced aggregation [61].

ZnO NPs for sunscreens (50 nm) were obtained in a dispersed state by including poly(aspartic acid) during reaction of zinc acetate and sodium hydroxide [62]. Humic acid-derivatized TiO_2 and fullerene NP are stable due to repulsive steric interactions, whereas larger natural organic matter (NOM) promoted aggregation by bridging [33,63,64]. Organosilanes are often used for covalent derivatization of surface hydroxyl groups to make NP stable in organic solvents, e.g. hydrolyzed decyltrimethoxysilane on titania makes hydrophobic particles stable in toluene [65].

The coating of NP with the specific types of ligand determine their stability in solvents, e.g. coating with citric acid and cetytrimethylammonium bromide lead to stability in water, whereas, thiol-based ligands confer stability in organic media [66–68]. Proper tuning of the ratio of surface hydrophobic (using decyltrimethoxysilane) and hydrophilic (using 3-aminopropyltrimethoxysilane) groups provide redispersion of TiO_2 in different solvents [69–71].

3.2.4. Non-aqueous systems

Over the past two decades, there has been considerable research in the use of nonaqueous solvents as the medium for NP synthesis [72,73]. Mostly metal oxides, but metal sulfides and metal nitrides have been synthesized [74]. Typical sources of the metal are from metal halides, metal alkoxides, metal acetates and metal acetonates. Solvents include alcohols, amines, hydrocarbons, ketones and typical temperatures of synthesis range from 50 to 250 °C. The organic solvents play an active role in the synthesis, often acting as the oxygen source (parallel to the role of water). M-OH and M-OR are intermediate species, prior to the formation of M-O-M bonds. Several strategies are reported for making stable dispersions of NPs in organic solvents, using the surface coordination concept, with surfactants, coordinating solvent or surface groups (e.g. chloride, other than hydroxides).

Using titania as an example, the diversity of synthetic routes to product is illustrated. Reaction of TiX_4 and $Ti(OR)_4$ with trioctylphosphine as surfactant at 300 °C formed 10 nm (size dependent on the halide, X) particles [75]. These particles do not have surface hydroxyl groups. The reaction between $TiCl_4$ and benzylalcohol produced highly crystalline anatase particles at temperatures of 40 °C [76]. The size of these particles varied from 4 to 8 nm depending on the temperature [76]. $TiCl_4$ in benzylalcohol-ethanol formed TiO_2 NP at temperatures of 80 °C [77]. Within an hour, the particle size was 2.3 nm, and increased to 8 nm after 8 h, with crystallinity being high around 6 h. These particles aggregated in a hydrophobic solvent, but dispersed well in water due to the surface being positively charged (low pH) [77]. To make NPs made in organic solvents water-dispersible, polar stabilizers (such as malic acid and glycine) need to be added to the organic reaction mixture, e.g. with glycine, highly crystalline anatase recovered from the organic solvent could be redispersed in water with 45 wt% loading [78]. C-undocecylcalix[4]-resorcinarene capped anatase titania nanoparticles have been synthesized, could be isolated and redispersed in other solvents[79].

Heating dilute solutions of $TiCl_4$ and diisopropyl ether in CH_2Cl_2 at temperatures of 80-150 °C led to phase pure unaggregated anatase, with chloride and isopropoxide surface groups, which help stabilization of these NPs and redispersion in other organic solvents [80]. Similar strategy was successful in synthesis of silica-titania, and tin oxide NPs [81,82].

Nonclassical routes are most likely for NP formation in organic solvents. Reaction of titanium butoxide and oleic acid at 250 °C led to an intermediate state of titania nanorods, formed by attachment of truncated Wulff bipyramids, which subsequently fractured to TiO_2 NPs [83].

Solvents such as t-butanol help in dispersibility by binding to the surface of the NP, as exemplified for NiO particles of sizes 2.5 to 5 nm, which are dispersible in ethanol, even after drying [84]. Surfactants such as oleic acid are necessary to stop NP aggregation.

Zirconia NPs functionalized with surface polymerizable vinyl groups (3-methacryloxypropyltrimethoxysilane) facilitated incorporation as individual NPs into PMMA and polyurethanes [85,86]. Oleylamine bonded to surface carboxylates on zirconia and hafnia assisted in dispersion of the NPs in nonpolar solvents [87]. High concentration of antimony-doped tin oxide decorated with oleylamine could be dispersed in THF and $CHCl_3$, but similar dispersions could not be made with oleic acid [88].

With hafnia and zirconia, protonation of the carboxylate group on the surface followed by binding of a positively charged amino acid stabilizes the dispersion electrostatically and makes possible the transfer from apolar ($CHCl_3$, toluene) to polar solvents (alcohols, acetone, DMSA, acetonitrile) [89].

Magnetite NPs prepared in hexane using oleic acid as surfactant upon treatment with polyethylene glycol methyl ether-poly (Є-caprolactone) amphiphilic block copolymer, and upon subsequent ring-opening polymerization of Є-caprolactone could be transferred to water phase, with increasing PEG block lengths promoting better transfer [90].

Polyols (e.g. ethylene glycol, diethylene glycol, triethylene glycol, tetraethylene glycol) can reduce metal salts to metal particles, act as high boiling solvents to facilitate the reduction, and also provide a surface coating to avoid aggregation. Magnetite NPs synthesized in liquid polyols are readily dispersed in water due to the polyol surface coating [91].

4. Aggregation upon drying

In many applications, it may be necessary to isolate the particles for further development. It is generally true that once particles are isolated from the solvent, then it is difficult to redisperse the particles. Drying leads to aggregation due a multitude of factors [54]. Colloidal processing is extensively practiced for ceramic fabrication, and involves drying of films containing NP [92]. Both physical and chemical effects are involved in the drying process.

4.1. Physics of drying: capillary forces

The physics behind drying is quite complex, since drying leads to many stresses. Liquids transported from internal to external parts of porous particles can cause compression of a 2D-solid network as drying occurs [92]. Compressive stress due to liquid evaporation in the capillary pores is related to the capillary pressure given by $P = 2\,\gamma\cos(\theta)/r$, where γ is the surface tension, r is related to the meniscus size, and θ is the contact angle between solvent and the solid surface [93]. The capillary forces can overcome the repulsive forces and bring particles together. Capillary induced tensile stress upon drying leads to cracking of films of α-Al_2O_3. Capillary induced tensile stresses are irreversibly dependent on particle size. The capillary tensions can also be sufficient to break up strongly aggregated clusters [94,95].

Drying of a suspension of nanocrystalline yttria-stabilized zirconia (primary particles 7–8 nm, but aggregated into 10–50 nm) has provided information about the evolution of the agglomerate structure [96]. Agglomeration begins as soon as liquid evaporates due to increasing concentration of the particles. The increase in concentration of dissolved ions upon liquid evaporation can minimize the electrostatic repulsive force, promoting agglomeration, even before capillary forces set in. Under conditions close to IEP, agglomerates tend to be sheet-like (diffusion-limited), whereas far from IEP, rounded structures form from chainlike structures (attachment-limited). Closer to IEP, primary particles are sticky, whereas away from IEP, the charge on the particles can keep the particles apart. At the final stages of drying compressive forces (can be as high as ~400 MPa for pore radii of 5 nm and surface tension of 1 J/cm^2) pull together the particles, whereas tensile forces can lead to cracks in the powder. The capillary forces promoting aggregation upon drying of NPs are due to the presence of liquid between the particles. These capillary forces are minimized if the particle surfaces are hydrophobic. With complete drying, agglomeration sets in and difficult to stop or reverse.

Heat treatment of NPs promote sintering due to stress between the NPs that promotes mass transport [10]. Presence of salts can alter electrostatic interaction between particles during drying. Drying of SiO_2 NPs from a salt solution led to residual stresses from salt bridging that influenced the packing of the dried particles [92]. The electrostatic interactions between the NPs can be minimized by short chain steric additives, instead of salts, as well as working near the IEP pH range [92].

4.2. Types of drying

The specific conditions during the drying process can lead to different sizes of aggregates. With silica colloids, oven drying led to strongly interpenetrated, robust aggregates of ~100 μm. Spray drying leads to more fragile clusters with less interpenetration and smaller particle size of ~20 μm. The rate of drying also influences final morphology, with slow drying (oven drying) leading to compact structures, whereas, fast drying (spray drying) leading to more open fractal structures [97].

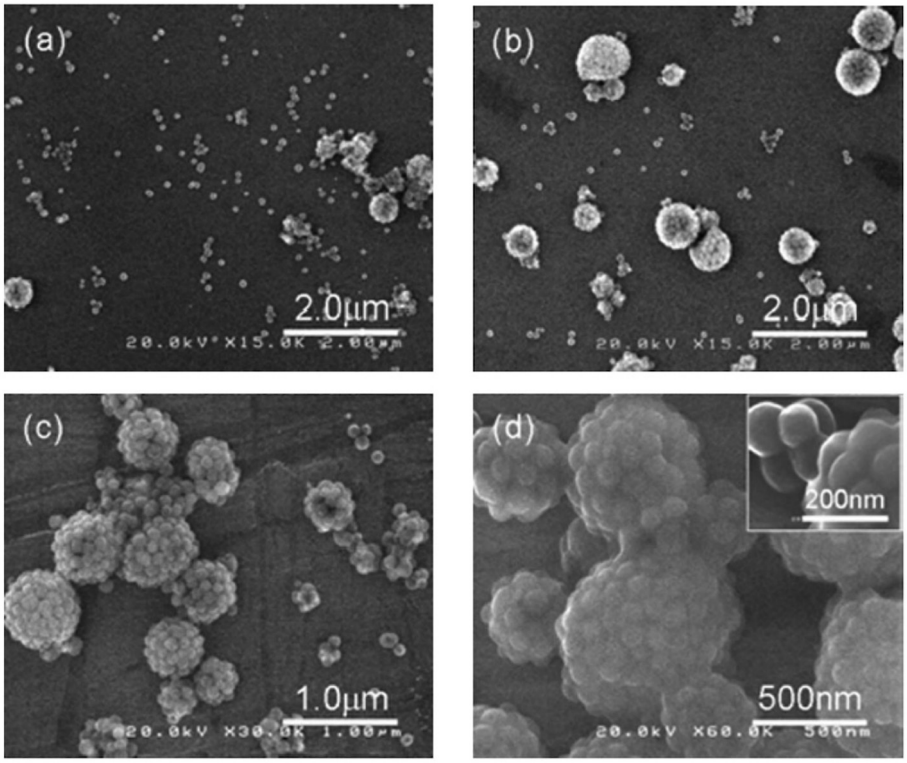

Fig. 6. SEM images of silica NPs with a nominal size of 85 nm upon low-pressure spray drying (40 Torr) at (a) 200 °C, (b) 400 °C, (c) 800 °C (d) 1000 °C. (taken from Reference [98]).

Spray drying involves the atomization of the NP suspension into a hot drying medium, and the morphology of the dried particles depends on the size of the NP, the droplet size, viscosity, temperature, pressure and gas-flow rate [98,99]. Low pressure spray-drying of Na^+-stabilized silica colloids in various size ranges 20–30 nm, 40–60 nm and 70–100 nm has been reported [98]. Fig. 6 shows the particle sizes as a function of drying temperature. For particle size in the range of 70–100 nm, mostly isolated dispersed NP, with a few aggregates were observed upon drying at 200 °C (pressure of 40 Torr), whereas with increase in drying temperature, the number and size of the aggregates increased. For the 20–40 nm particles, aggregates are formed, and correlated with the higher surface potential of the smaller particles. Lower pressures of 20 Torr, 200 °C, 0.4 wt% and gas flow rates of 2 l/min produced isolated 85 nm particles for the 70–100 nm particles, whereas at atmospheric pressure, only aggregates were observed [98]. It was proposed that at the low pressures, the osmotic pressure is larger than the Laplace pressure, leading to fragmentation into smaller droplets. It was noted that for these SiO_2 NP, higher pH favored dispersion, with the optimal results at pH 8.52, reflecting the increase in ZP, and higher electrical repulsive forces. At pH of 11.27, even though the ZP increased, agglomerates were observed, since particles dissolve at the high pH, and the oligomeric silicate can act as bridging ligands between particles.

The structure of aggregates formed by spray drying of SiO_2 NP (primary particle size of 200 nm) was independent of the terminal functionality of the surface groups (epoxy, CH_3, NH_2 or OH), though the mechanical properties of the dried sample differed with the surface-bound ligand [100]. The aggregate size as well as its internal structure determines the micromechanical properties. For example, with epoxy end groups, bridges between particles are formed as compared to direct bonding between the particles with the other functionalities, leading to aggregates with more plastic deformation behavior.

Freeze-drying (lyophilization) is also another method for drying particles, and common in the biotech industry for DNA, proteins and peptides. Freeze-drying cycle typically has three steps: freezing (~ -40 °C), primary drying by sublimation of the ice under vacuum, and secondary drying to remove unfrozen water (25-50 °C). During the freezing step, aggregation can occur due to increased concentration of the NPs, as well as the increase in ionic strength in the cryo-liquid can alter the zeta potential and promote aggregation. The labile NPs also need to be protected against the mechanical stresses developed during the freezing and desiccation steps. Cryoprotectants, usually sugars are often used, these form a glassy state with 15–30% water and extensive H-bonding upon freezing. NPs are dispersed in these amorphous pools and are protected. The solids isolated from freeze drying can be stored for long periods, without aggregation and ready redispersion in water. The primary application of freeze drying is for biologics, and has been well documented [101–103]. We discuss here a few examples of inorganic NP systems that have been studied with freeze-drying. Freeze drying of 18 nm PEG-Fe_3O_4 (magnetite core – 9 nm, polymer sheath- 9 nm) particles produced redispersible NP suspensions stable for 20 months [104], with the poly(ethylene glycol) gallol providing protection against irreversible aggregation during the drying step. Silica particles were modified by reaction of surface silanol groups with N-(2-aminoethyl)-3-aminopropyltrimethoxysilane, thereby generating cationic amino groups tethered to the surface [105]. Upon freeze-drying, significant aggregation took place, and could be completely avoided if a cryoprotectant such as trehalose or glycerol was included during the freeze-drying step. The sugars, by H-bonding with surface silanol groups, inhibited permanent particle aggregation.

4.3. Surface modification effects on drying

A novel approach to obtain controlled heteroaggregates upon drying is by adjusting the surface charge of two different NP to opposite charges that promote attraction [6]. Using formic acid to adjust the surface charge of TiO_2 and SnO_2 to positive and negative charge at the same pH, TiO_2-SnO_2 heterojunction particle networks could be formed upon vacuum annealing, with enhanced photo driven charge separation [106].

In case of NPs with surface hydroxyl groups, such as silica, reactive condensation of surface – OH groups between neighboring particles can lead to covalently bound aggregates. Resulting particles are disoriented at the surface, and it is difficult to establish electrical double layers around the NPs. Application of external energy such as ball milling and sonication can break apart such aggregates, but is often temporary and re-aggregation occurs. Even gentle drying techniques such as freeze drying, supercritical fluid drying and azeotropic distribution does not typically make redispersible particles with NPs with surface hydroxyl groups [54].

5. Redispersing strategies

NIST provides 26 protocols for preparation of nanoparticle dispersion, size measurement, nanotoxicology testing, sample preparation for electron microscopy and elemental analysis focusing on TiO_2, CNT, silver and gold NPs [107].Table 2 provides examples of different strategies taken to disperse NP, all exemplified with titania NPs [54].

5.1. Dispersing medium

Different solvents influence aggregation of NPs in profound ways. The important properties of the solvent in influencing NP aggregation are its coordinating ability (surface complexation), viscosity (lower viscosity promotes increased diffusion) and dielectric constant (lower values will decrease the repulsive interactions). Influence of solvent on NP stability was studied for three NPs: anatase (26.9 ± 4.9 nm length, 16.9 ± 3.5 nm width), goethite (α-FeOOH, 100 ± 39 nm length, 11.5 ± 4.1 nm width) and ferrihydrite (Fe_5HO_8 $4H_2O$, 6.4 ± 1.3 nm

Table 2
Strategies reported for redispersibility of NPs, exemplified by titania NP. (adapted from Reference [54]).

Stabilization Method	Stabilization mechanism	Reference
External energy	Two mechanical dispersion methods, ultrasonication and milling showed that sonication could generate the primary particles, even for concentrated dispersions.	[111]
Peptization	Synthesis of TiO_2 NP by controlling the pH during hydrolysis of titanium isopropoxide to pH ~ 2. Low pH leads to surface protonation and particle repulsion	[164]
Doping	Al^{3+} doping of TiO_2 (both bulk and surface) retards coalescence of TiO_2 during calcination by reducing energy.	[53]
Polymer dispersants	Polyethyleneimine adsorbed on TiO_2 NP imparts a positive charge leading to well-dispersed suspensions.	[57]
Surface modification (aqueous)	TiO_2 NP coated with 2, 3-dimercaptosuccinic acid made possible dispersion in water at pH 6–10, arising from repulsion of the negatively charged NP	[165]
Surface modification (organic)	4-tert-butylalcohol adsorbed on TiO_2 NP during synthesis made possible dispersions in dimethylformamide	[126]
Pickering emulsions	TiO_2 NP (6 μm) helped stabilize water in oil emulsions (pH 3) with cyclohexane and n-hexane in the presence of salts or hydrophobic coupling molecules, e.g. alkyl phosphates	[166]
Foam stabilization	TiO_2 NP adsorbed at the air-water interface stabilized foams with sodium dodecyl sulfate and cetyltrimethyl ammonium bromide. These surfactants generate the TiO_2 hydrophobic by surface adsorption	[167]

length, 4.9 ± 1.0 nm width) in four neat solvents, water, isopropyl alcohol, acetic acid and THF [108]. The particles were all synthesized in water, and transferred to the other solvents by dialysis. Characterization techniques included cryo-TEM and dynamic light scattering to measure aggregation. Suspensions in water formed the smallest and least compact aggregates, whereas THF formed the largest and most compact aggregates. Uniqueness of water in stabilizing the smallest NPs stems from its high dielectric constant, coordinative and H-bonding abilities.

Success of resuspension of commercial NPs depends on the type of NP, e.g., metal versus metal oxide, and in the solvent medium that the dispersion is occurring [1]. For example, with Au, Co, Fe_2O_3, TiO_2 and CeO_2 NPs, the metals were unstable in all media, whereas the oxides were more stable in tetramethylammonium hydroxide (TMAOH) as compared to water or PBS buffer. This is exemplified in Fig. 7 ab, which shows the stability and particle size of Fe_2O_3 in aqueous media with buffers (PBS) and TMAOH, whereas Fig. 7 c shows the stability of three different oxides (TiO_2, Fe_2O_3 and CeO_2) in TMAOH [1].

5.2. Mechanical forces

Physical forces such as ultrasound and ball-milling will reduce agglomeration [109,110]. Ultrasonic radiation generates collapsing cavitants, which promote interparticle collisions, with the ultrasonication amplitude being an important experimental parameter for determining the stability of the suspension [111,112], and has been demonstrated with TiO_2 in water [110]. Surfactants are often added to stop the reaggregation once the energetic perturbation is removed [54].

Analysis of the drying protocol of precipitated silica showed adverse effects on their redispersion using ultrasonication. Precipitated SiO_2 with primary size of 12.6 nm formed 300 nm clusters, which packed into 7 μm hard aggregates and 116 μm soft aggregates, prior to drying. If the samples were not dried, sonication can break the silica down to the hard aggregates of ~3.5 μm. If samples are dried at 150 °C, then the soft aggregates do not break down completely upon sonication, leading to ~11 μm aggregates, indicating hardening of the soft aggregates [113].

Commercial dry samples of NP are often aggregates (3 μm) and commercial TiO_2 particles (500 nm aggregates) could not be broken up into the primary particles (<typically 100 nm) by sonication, dispersants, organic solvents or pH manipulation [114]. This is not surprising considering the discussion above related to NP aggregation with drying. Fresh wet-flocculated hematite particles were redispersed into the primary size by sonication [114]. Even long-term storage of suspension of NP leads to aggregation e.g. lab-synthesized 85 nm hematite stored for one month followed by dispersion in water led to 110 nm particles and 130–160 nm irreversible aggregates. It was predicted that metal oxide NP with size range of 1 nm −10 μm will aggregate even when stored as dry powders [114].

SiO_2/TiO_2 composite NPs prepared were bead-milled to nearly their primary particle size by breaking up the necked structure in *N*-methylpyrrolidone with surface modifying ligand phenyltrimethoxysilane [115]. This group also reported that mixtures of polyethyleneimine and fatty acids can stabilize TiO_2 NP into toluene [115].

5.3. Manipulating capillary forces

Manipulation of the capillary forces during drying led to organized NP on surfaces. As liquid between particles evaporate, particles are pulled together by capillary forces, and especially strong for large (500 nm) hydrophilic particles [116–118]. Inter-particle attraction via capillary forces increases if the contact angle between the particle and surrounding liquid decreases [119]. Since the magnitude of capillary forces is directly dependent on surface tension, changing solvent from water to ethanol results in a three-fold reduction in capillary forces [120,121]. Also, by replacing water with isopropanol, a liquid with a lower surface tension decreases the capillary forces [119]. Fig. 8 shows that large areas of well-ordered unaggregated 500 nm silica particles was obtained upon drying on glass coated with a polycation. This process could be further improved by inclusion of small particles (30 nm), which positioned between the larger ones and provided steric repulsion, and/or deposition of a layer of macromolecules (polycations) on top of the silica deposit, with good dispersion evident even upon drying at 450 °C for 3 h [116]. Protonated polyallylamine chloride, a polycation adsorbed on the surface of the silica particles increased the contact angle and decreased capillary forces, leading to non-aggregated particles [116]. Similar effects have also been noted in suspensions, 6 nm ZrO_2 NP stabilized 600 nm silica particles [122] and 8 nm magnetite particles stabilized 1.45 μm magnetite particles [123].

Coating the silica nanoparticles with cationic polyelectrolytes also promoted strong repulsive forces, that negated the effects of the capillary forces during drying [124]. The surface charge on rough and smooth SiO_2 NP (137 nm) can be changed from negative to positive by derivatization

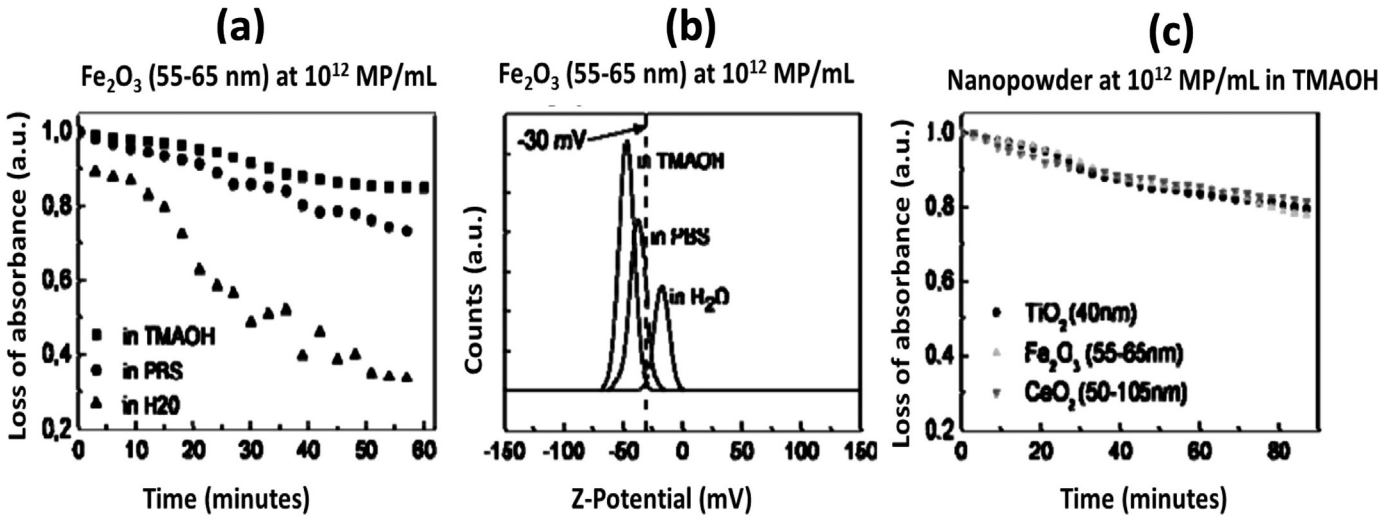

Fig. 7. Stability of resuspended Fe_2O_3 NPs in different aqueous media. (a) Loss of absorbance due to particle settling out, most pronounced in water (b) Zeta potential graphs again demonstrating instability in water (c) TiO_2, Fe_2O_3, and CeO_2 NPs all exhibit similar settling patterns in TMAOH.
(taken from Reference [1].)

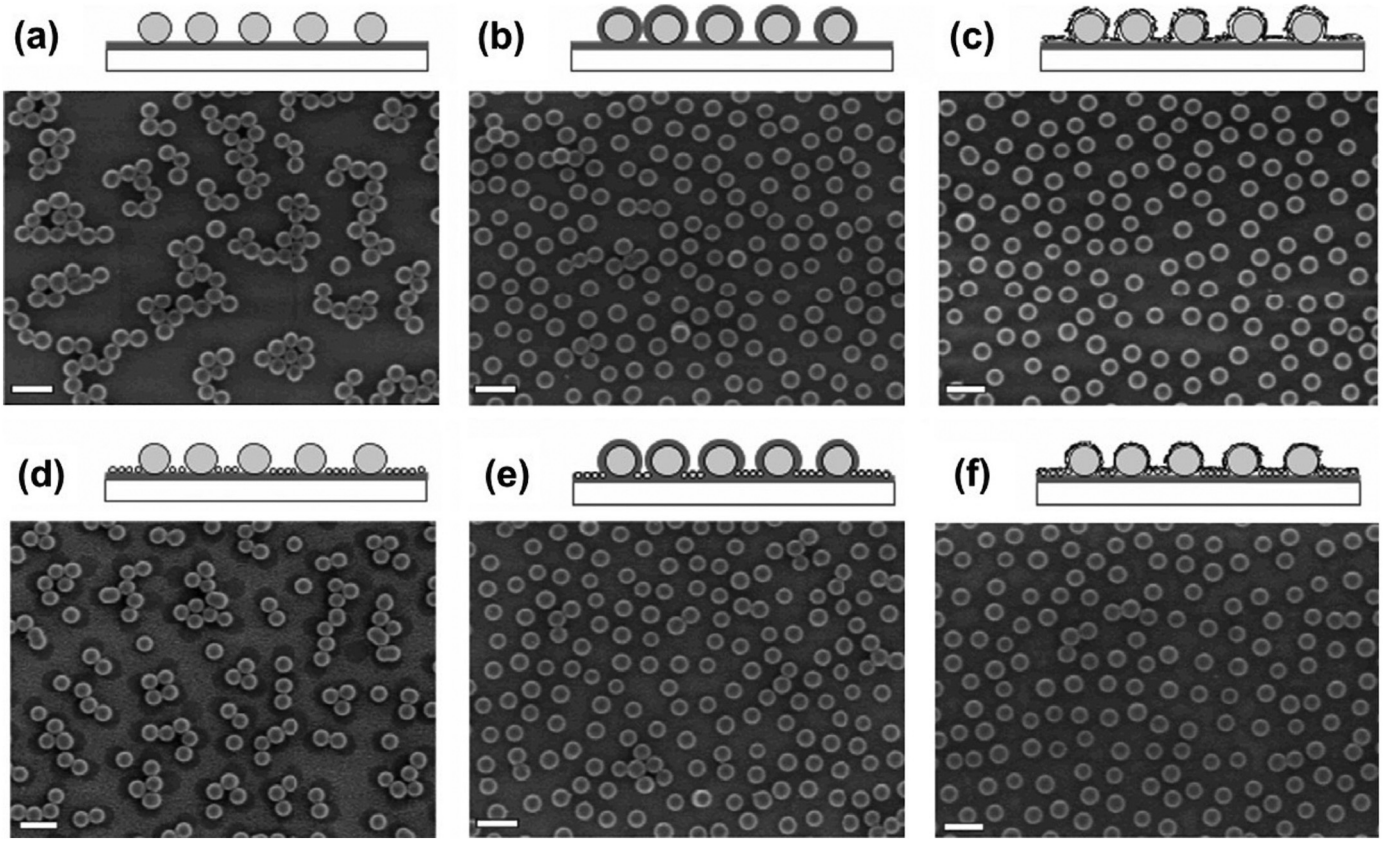

Fig. 8. Top bars in each figure is a schematic representation and the figures are SEM images of 500 nm silica deposits on glass substrates previously covered by PAH. The 500 nm colloid deposition step was followed by the adhesion of 30 nm colloids in conditions d, e and f. In some cases, adherent colloids were covered by an additional layer of PAH (b and e) or albumin (c and f) before drying. The scale bar is 1 μm.
(taken from Reference [116]).

of –OH groups with (6-aminohexyl)aminopropyltrimethoxysilane, and these particles pack in an ordered, non-closed-packed arrangement on a functionalized gold surface. Aggregation from capillary forces can be decreased for particles with rough surfaces via friction, as well as covalent bonding with the substrate. Rough particles are bound more strongly to the surface due to additional friction forces, which decreases lateral mobility [13].

5.4. Manipulating surface characteristics

Ball milling of calcium carbonate in the presence of sodium salt of poly(acrylic acid) led to stable aqueous dispersions of 10–100 nm particles, with the negative charge of the surface adsorbed acrylate providing repulsion between particles [125].

With SiO_2 particles, silanol group condensation between particles lead to aggregation [105]. Derivatization of these silanol groups with amino groups (reaction with aminoalkylsilanes) giving them a positive charge makes them more amenable to dispersion.

Surface modifications of the NPs during synthesis (prior to particle isolation) can also lead to dispersed particles [54]. TiO_2, coated with dopamine or catechol is stable in water and organic solvents, respectively [126]. TiO_2, coated with butoxy groups during synthesis can be dried and upon dispersion in water leads to a stable suspension since the butoxy linkages are hydrolyzed. Covalent surface modification with organosilanes is a common practice with particles with surface OH groups.

Well dispersed TiO_2 NP distributed in polymer matrices without aggregation was accomplished using different surface modifications after synthesis, and are shown schematically in Fig. 9 [127]. The TiO_2 NP (2–6 nm) prepared by hydrolysis of $TiOCl_2$ with water/ethanol were isolated as a wet cake by centrifugation. All derivatization procedures were carried out on the wet material. Particles washed with ethyl acetate and propionic acid were dispersible in water up to 5 wt%. Treatment with propionic acid and C_3, C_6 and C_{10} amines led to particles that were dispersible in water and 2-propanol (C_3 amine), $CHCl_3$ and toluene (C_6, C_{10} amine). These amine modified TiO_2 samples could be incorporated in polymer films with polar groups (poly(bisphenol-A and epichlorohydrin and a copolymer of styrene and maleic anhydride) to make clear films, but nonpolar polymers (polystyrene) did not form clear films [127].

There are other strategies to make redispersible particles upon drying. Strong acids protonate oxide surfaces, resulting in electrostatic

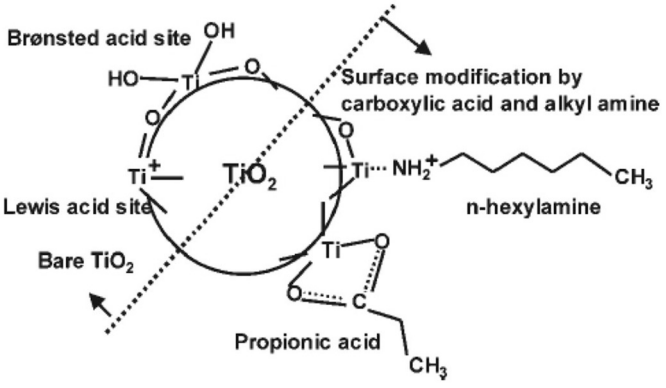

Fig. 9. Different types of surface groups on bare TiO_2 and acid and amine-modified TiO_2.
(taken from Reference [127].)

repulsion between particles, as well as resulting in breaking of oxonation bonds [128]. For example, TiO_2 (prepared from $TiCl_4$, particles sizes of 5, 8 and 4 nm) treated with 2 M $HClO_4$, HNO_3 were dispersible after drying at 150 °C, with the remaining acid in the dry sols preventing aggregation of the particles upon redispersion. Still some aggregation took place, with particle sizes of 36, 32 and 79 nm, with $HClO_4$ being the better peptizing agent. If the acid is neutralized, then the particles aggregate into much larger sizes during drying [129].

Another strategy for making redispersible SiO_2 NPs (25 nm) was to coat it with D-mannitol in water/ethanol, followed by spray drying [130]. Upon drying, large micron-sized hollow spheres were obtained. The mannitol because of its hydroxyl groups form H-bonds with the surface of the silica particles, keeping them apart. Upon redispersion of the micron-sized particles in water, the mannitol dissolves and the primary particles were recovered. It is reported that 40 wt% SiO_2 NP (not dried, but in a wet precipitate form) if mixed with polybutylene terephthalate in CF_3COOH can be dried under vacuum, and remain re-dispersible even after being in a dry state for 5 months [131].

6. Aggregation relevant applications

There is a long history of human use of NPs, though the nanoscale properties were not recognized. During more recent times, examples include the use of SiO_2 NPs for rubber enforcement, Ag NP for antibacterial technology, various NPs in automotive industry for tires, fillers in the car body and metallic and nonmetallic paint finishes, TiO_2 NPs in dye-sensitization to make solar cells, and TiO_2 and ZnO in cosmetics [132,133]. In practical application, such as in paints, advantage is taken of increasing viscosity to minimize NP aggregation by minimizing particle movement [36].

Antibiotic, antistatic, light tolerant textiles can be fabricated with the aid of NPs, which can be soaked into the garment e.g. ZnO, or directly synthesized within the textile such as with silver [134–136]. NP aggregation is minimized by cross-linking the particles into a polymer web [4]. Silica NP incorporated into polypropylene filaments improve flame retardancy since it raises the limiting oxygen index (the minimum amount of oxygen necessary to sustain combustion) from 18 to 22% (note oxygen in air is 21%) [137]. Cotton fabrics impregnated with silica, alumina, titania and zirconia sol gels followed by thermal treatment provided thermal and fire stability to the textiles [133,138]. Co-electrospinning of polyurethane and ZnO NPs (24–71 nm) resulted in fibers with isolated ZnO NPs with reduced transmission for both UVA and UVB light, however air and moisture vapor transport decreased [139].

For heterogeneous catalysts, the size of the NP is important, but since these experiments are done under high temperature, the NP tend to sinter, minimizing activity [6]. To alleviate this problem, NP can be made in a core-shell configuration, with the shell protecting NP aggregation. Examples are Pt and Ag NP in mesoporous silica, the latter could be heated to 500 °C without coarsening [140,141]. For environmental remediation, zerovalent iron particles are used since these NPs can decompose chlorinated compounds, as well as immobilize heavy metals. However,

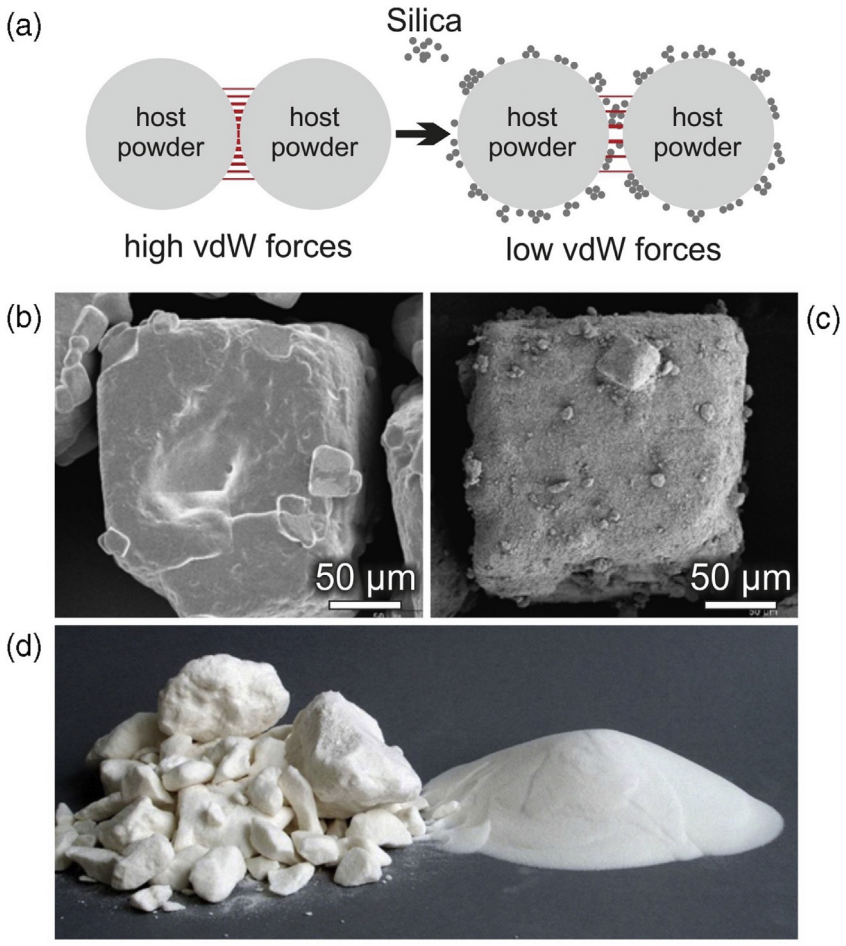

Fig. 10. (a) Use of surface adsorbed nanosilica to reduce van der Waals attractive forces, (b,c) SEM images of NaCl crystals without (b) and with silica (d) Demonstration of using silica as a flow aid, picture on right with silica.
(taken from Reference [133].)

these NPs can aggregate in groundwater and deposit, thereby neutralizing their activity. The aggregation is alleviated by encapsulating the particles in a silica matrix or by surface modification with polyelectrolytes, though there are still technical issues with polydispersity in the zerovalent iron NPs, especially at high concentrations [142]. NPs are often stabilized on supports, but the synthesis of such composites is not always straightforward. For example, already synthesized AuNP (2 and 10 nm size) aggregated upon introduction to the medium (basic solution of tetramethyl orthosilicate) for preparing silica aerogels. It was found that in the presence of polymers such as poly(vinylpyrrolidone) and poly(vinylalcohol), the AuNPs could be incorporated into multicentimeter sized silica aerogel monoliths without any aggregation [143].

Tire performance with highly dispersible silica was better as compared to precipitated silica as manifested in wear resistance, rolling resistance and wet grip [144]. However, the binding of hydrophobic rubber and hydrophilic silica requires the use of silane coupling agents, and appropriate mixing at high temperatures. Nanoscale TiO_2, ZrO_2 SnO_2, P_2O_5 are added as nucleation agents for manufacturing glass [133]. With 20 nm P_2O_5 added as a nucleation agent to lithium silicate glass, it was noted that the glass showed superior mechanical properties with flexural strength of 290 MPa and microhardness of 620 HV [145].

Oxide dispersed strengthened (ODS) metal alloys are prepared by high energy milling of ferritic matrix powder and Y_2O_3 (staring size 1 μm along with agglomerates of 10 μm) resulting in homogeneous dispersion of sub 10 nm oxides within and around grains [146]. Milling at kilogram levels can be done in vacuum and inert atmosphere. The strength of ODS alloys (FeCrAl) increased by 40 MPa at 20 °C and 70 MPa at 1000 °C, factors of 5–10% and 4000% respectively [133].

Calcium silicate hydrate (CSH) nanoplates added as seeds can improve the properties of cement [24,133]. Use of hydrophilic phosphate comb polymers orients the platelets of CSH aggregate in an edge-to-edge fashion by a combination of adsorption through carboxylate functionalities as well as steric repulsion through hydrophilic segments [147]. The resulting concrete hardens at lower temperatures, making possible structures with lower energy costs.

Fig. 10 shows how silica can work as a flow aid. Nanoscale silica (<50 nm) at loading levels of 1 wt% can coat surfaces of host powders [133,148], reducing the VDW attraction between particles, enabling free flow and anticaking. Similar strategy has been practiced for enabling ready flow of toners for laser printers using fumed silica and titania. Silica NPs has also been shown to keep soft powders such as fats, waxes and emulsifiers from caking, but used at a higher loading level of 5 wt%. Use of porous silica for flow of wet powders has also been realized with the silica adsorbing the liquid between the host powder particles and reducing the capillary forces between the particles, facilitating the flow. Fire extinguishing powders of size 45 μm that flow readily are made by milling with 0.5–1 wt% of silica and prevents the particles from agglomerating. The milling step is critical, since it is during this process that the NPs attach to the larger particle, and the milling also serves to break up the aggregates of NPs. There is an optimum amount of NP that is needed, too much of it will increase the tensile strength between the large particles and impede flow [148].

Magnetic NPs, in particular, magnetite (Fe_3O_4) and maghemite (γ-Fe_2O_3) are useful for clinical applications, and many studies exist on making stable suspensions in aqueous and organic media and is the subject matter of recent review articles [149,150]. Magnetic fluids are colloidal (~10 nm) single domain magnetic NPs, coated with surfactants, e.g. oleic acid (bidentate ligand to iron), and dispersible in water and nonpolar (mineral oil) media [151,152]. Fe_3O_4 NPs stabilized with oleic acid are stable in organic solvents, including toluene, hexane, $CHCl_3$. These NPs can be made water compatible by ligand exchange of oleic acid with dopamine and dihydroxy-1,3-benzenedisulfonic acid salts (Tiron) [153]. Two to three nm Au particles could be electrostatically attached to the amine group of the dopamine chelated iron oxide NPs to generate water dispersible Au-Fe_3O_4 hybrid NPs [154]. Twenty to forty nm Fe_3O_4 NPs stabilized with citrate dispersed in water, and were stable to aggregation because of electrostatic repulsions [155].

Nanoclays are incorporated in polymers to improve gas barrier properties as well as increase mechanical strength, stiffness and heat resistance. The starting material for these approaches uses naturally occurring clays, which are micron-sized particles made up of nanometer-sized sheets. In order to get the beneficial properties of the clay-polymer composite, the clay has to be delaminated into the nanosheets (dimensions of nm in the thickness of the sheet), and well dispersed within the polymer. Typically, the approach is to intercalate long-chain organic molecules within the sheets to make the material hydrophobic, and use this as a starting material. There are three methods for incorporation into the polymer: in situ polymerization, in which the monomer gets incorporated into the sheets and cause exfoliation during the polymerization, a polymer/solvent solution-induced intercalation, which causes swelling of the clay and dispersion, and a melt processing that promotes exfoliation during the melt process [156–158]. Fig. 11 shows a truck cargo bed made with nanoclay-polymer composite.

Fig. 11. Use of nanoclay-polymer composite materials on a truck bed.
(taken from Reference [156].)

Nanoscale ceria coated on diesel particulate filters are extensively used for reducing particulate emissions. The CeO_2 NPs of size 10–20 nm are stabilized by electrostatic charge as a colloidal suspension, and available commercially. Coatings on the filter at weight percentages of 17 wt% CeO_2 are reported [159]. Nanoscale ceria also finds use as a fuel additive for reducing diesel emissions. The challenge in this technology is to insure that the ceria remain dispersed in the fuel for extended periods. The stability is dependent on the concentration of ceria as well as the use of appropriate dispersants. It is reported that with oleic acid as dispersant, 10 ppm CeO_2 of 40–50 nm size was stable in the diesel for at least eight weeks [160].

Nanofluids, which are dispersions of NP, are being examined for enhanced cooling by heat dissipation in heat exchangers. Properties such as thermal conductivity, viscosity, density are increased and specific heat is decreased. It has been proposed that thermal conductivity exhibits a bell-shaped curve with aggregation, with the isolated NPs or large aggregates having lower conductivity than an optimum sized aggregate of the NP [161]. Metals, oxides, nitrides, metal carbides, CNT have all been studied in solvents such as water, ethylene glycol and oils [161]. The NP dispersion can be prepared from a dry powder using high shear and ultrasound, the latter being very effective with a horn ultrasonic vibrator [162]. A novel method of dispersing TiO_2 NPs in water was accomplished using a high pressure homogenizer [163]. An alternative method is to generate the NP within the liquid by using surfactants, common ones being sodium dodecylsulfate, sodium dodecylbenzene sulfonate, oleic acid, cetyltrimethylammonium bromide, dodecyl trimethylammonium bromide, sodium octanoate, hexadecyltrimethyl ammonium bromide, polyvinylpyrrolidone and Gum Arabic [161].

7. Conclusions

In summary, this review demonstrates the burgeoning applications of NPs in a wide variety of applications, including consumer products, energy, chemical/petrochemical products and in medicine. It is also apparent that the synthesis of NPs and keeping them in a non-agglomerated state or carrying out controlled aggregation for specific applications requires considerable chemical and physical insight. Much research has been carried out in this area with metal oxides, including silica, titania, zinc oxide, ceria, iron oxide, and metals, particularly silver and gold. Gas phase synthesis has the potential for scale up to kg/h levels, but often resulting in aggregated particles. Manipulating the temperature and pressures within the reactor for gas phase synthesis is necessary to get optimal size distribution. Though, mechanical grinding methods are often necessary for obtaining NPs. Liquid phase synthesis provides better control of size and morphology. Exploiting the surface characteristics of the NP, including surface charge and functionality are often used for particle size control. Surface coating by polymers, surfactants, polyelectrolytes provide ways to thwart NP aggregation. Control of hydrophobic versus hydrophilic surface groups can make NPs stable in polar and nonpolar solvents. Many applications require that NPs prepared by liquid methods be isolated as a dry powder. Without any precautions, any drying process will lead to aggregates, primarily driven by the large capillary forces as liquids between the NPs evaporate. Several studies have investigated the fundamentals of the aggregation phenomena upon drying. If the agglomerates have strong NP-NP association, which is often the case, mechanical forces such as ball milling provide the only route to break up the agglomerates, but not necessarily to the primary particle size. Surface derivatization during the synthesis process can in some cases make redispersible NPs, and examples are provided. Redispersion becomes easier if all of the solvent is not removed during drying. There are numerous examples of real-world applications of NPs, and in each of these technologies, a thoughtful approach to avoid and/or control aggregation is important, and many such examples are presented in the final section. Many of these technologies also understand the limitations or advantages (in some cases) of aggregation. Proper dispersion of NP in matrices, e.g. polymers are relevant for the final desired physical properties.

There are outstanding issues associated with NP-based technology that merit further attention, including.

- Scale up of liquid-based manufacturing that provides control over particle size distribution and repeatability, with built-in cost efficiency.
- Issues of safety, both occupational safety during manufacture and during use by the consumer.
- Environmental impact of NPs, including effects on wildlife, fisheries, plant kingdom and agriculture.
- Impact of NPs on the water table, rivers and oceans.

Declaration of Competing Interest

The authors declare that they have no known competing financial interests or personal relationships that could have appeared to influence the work reported in this paper.

Acknowledgment

This work was partially supported by a NSF SBIR Award number [1841732].

References

[1] Casals E, González E, Puntes V. Reactivity of inorganic nanoparticles in biological environments: insights into nanotoxicity mechanisms. J Phys D Appl Phys 2012; 45:443001. https://doi.org/10.1088/0022-3727/45/44/443001.
[2] Lu Z, Yin Y. Colloidal nanoparticle clusters: functional materials by design. Chem Soc Rev 2012;41:6874–87. https://doi.org/10.1039/C2CS35197H.
[3] Stolarczyk JK, Deak A, Brougham DF. Nanoparticle clusters: assembly and control over internal order, current capabilities, and future potential. Adv Mater Weinheim 2016;28:5400–24. https://doi.org/10.1002/adma.201505350.
[4] Stavis SM, Fagan JA, Stopa M, Liddle JA. Nanoparticle manufacturing – heterogeneity through processes to products. ACS Appl Nano Mater 2018;1:4358–85. https://doi.org/10.1021/acsanm.8b01239.
[5] Hotze EM, Phenrat T, Lowry GV. Nanoparticle aggregation: challenges to understanding transport and reactivity in the environment. J Environ Qual 2010;39: 1909–24. https://doi.org/10.2134/jeq2009.0462.
[6] Xu L, Liang H-W, Yang Y, Yu S-H. Stability and reactivity: positive and negative aspects for nanoparticle processing. Chem Rev 2018;118:3209–50. https://doi.org/10.1021/acs.chemrev.7b00208.
[7] Cushing BL, Kolesnichenko VL, O'Connor CJ. Recent advances in the liquid-phase syntheses of inorganic nanoparticles. Chem Rev 2004;104:3893–946. https://doi.org/10.1021/cr030027b.
[8] Mansfield E, Kaiser DL, Fujita D, de Voorde MV. Metrology and standardization for nanotechnology: Protocols and industrial innovations. John Wiley & Sons; 2017.
[9] Kreyling WG, Semmler-Behnke M, Chaudhry Q. A complementary definition of nanomaterial. Nano Today 2010;5:165–8. https://doi.org/10.1016/j.nantod.2010.03.004.
[10] Kamiya H, Gotoh K, Shimada M, Uchikoshi T, Otani Y, Fuji M, et al. Chapter 3- characteristics and behavior of nanoparticles and its dispersion systems. In: Hosokawa M, Nogi K, Naito M, Yokoyama T, editors. Nanoparticle technology handbook. Amsterdam: Elsevier; 2008. p. 113–76. https://doi.org/10.1016/B978-044453122-3.50006-4.
[11] Jassby D, Farner Budarz J, Wiesner M. Impact of aggregate size and structure on the photocatalytic properties of TiO_2 and ZnO nanoparticles. Environ Sci Technol 2012; 46:6934–41. https://doi.org/10.1021/es202009h.
[12] Vikesland PJ, Heathcock AM, Rebodos RL, Makus KE. Particle size and aggregation effects on magnetite reactivity toward carbon tetrachloride. Environ Sci Technol 2007;41:5277–83. https://doi.org/10.1021/es062082i.
[13] Schmudde M, Grunewald C, Goroncy C, Noufele CN, Stein B, Risse T, et al. Controlling the interaction and non-close-packed arrangement of nanoparticles on large areas. ACS Nano 2016;10:3525–35. https://doi.org/10.1021/acsnano.5b07782.
[14] Sebastian V, Arruebo M, Santamaria J. Reaction engineering strategies for the production of inorganic nanomaterials. Small 2014;10:835–53. https://doi.org/10.1002/smll.201301641.
[15] Buesser B, Gröhn AJ. Multiscale aspects of Modeling gas-phase nanoparticle synthesis. Chem Eng Technol 2012;35:1133–43. https://doi.org/10.1002/ceat.201100723.
[16] Schulz C, Dreier T, Fikri M, Wiggers H. Gas-phase synthesis of functional nanomaterials: challenges to kinetics, diagnostics, and process development. Proc Combust Inst 2019;37:83–108. https://doi.org/10.1016/j.proci.2018.06.231.
[17] Tsantilis S, Pratsinis SE. Soft- and hard-agglomerate aerosols made at high temperatures. Langmuir 2004;20:5933–9. https://doi.org/10.1021/la036389w.

[18] Akhtar MK, Pratsinis SE, Mastrangelo SVR. Dopants in vapor-phase synthesis of Titania powders. J Am Ceram Soc 1992;75:3408–16. https://doi.org/10.1111/j.1151-2916.1992.tb04442.x.

[19] Schulz H, Mädler L, Pratsinis SE, Burtscher P, Moszner N. Transparent nanocomposites of radiopaque, flame-made Ta_2O_5/SiO_2 particles in an acrylic matrix. Adv Funct Mater 2005;15:830–7. https://doi.org/10.1002/adfm.200400234.

[20] Strobel R, Stark WJ, Mädler L, Pratsinis SE, Baiker A. Flame-made platinum/alumina: structural properties and catalytic behaviour in enantioselective hydrogenation. J Catal 2003;213:296–304. https://doi.org/10.1016/S0021-9517(02)00082-9.

[21] Loher S, Stark WJ, Maciejewski M, Baiker A, Pratsinis SE, Reichardt D, et al. Fluoroapatite and calcium phosphate nanoparticles by flame synthesis. Chem Mater 2005;17:36–42. https://doi.org/10.1021/cm048776c.

[22] Takashiri M, Tanaka S, Takiishi M, Kihara M, Miyazaki K, Tsukamoto H. Preparation and characterization of $Bi_{0.4}Te_{3.0}Sb_{1.6}$ nanoparticles and their thin films. J Alloys Compd 2008;462:351–5. https://doi.org/10.1016/j.jallcom.2007.08.054.

[23] Kelesidis GA, Goudeli E, Pratsinis SE. Flame synthesis of functional nanostructured materials and devices: surface growth and aggregation. Proc Combust Inst 2017;36:29–50. https://doi.org/10.1016/j.proci.2016.08.078.

[24] Rieger J, Kellermeier M, Nicoleau L. Formation of nanoparticles and nanostructures–an industrial perspective on $CaCO_3$, cement, and polymers. Angew Chem Int Ed Engl 2014;53:12380–96. https://doi.org/10.1002/anie.201402890.

[25] Lin MY, Lindsay HM, Weitz DA, Ball RC, Klein R, Meakin P. Universality in colloid aggregation. Nature 1989;339:360–2. https://doi.org/10.1038/339360a0.

[26] Bowers C, Dutta PK. Pentacarbonyl iron(0) in zeolite Y: structure and reactivity. J Phys Chem 1989;93:2596–603. https://doi.org/10.1021/j100343a069.

[27] Boutonnet M, Kizling J, Stenius P, Maire G. The preparation of monodisperse colloidal metal particles from microemulsions. Colloids Surf 1982;5:209–25. https://doi.org/10.1016/0166-6622(82)80079-6.

[28] Ohshima H. The DLVO Theory of Colloidal Stability. Electrical Phenomena at Interfaces and Biointerfaces: Fundamentals and Applications in Nano-, Bio-, and Environmental Sciences. John Wiley & Sons; 2012.

[29] He YT, Wan J, Tokunaga T. Kinetic stability of hematite nanoparticles: the effect of particle sizes. J Nanopart Res 2008;10:321–32. https://doi.org/10.1007/s11051-007-9255-1.

[30] Kim JY, Kim D-W, Jung HS, Hong KS. Influence of Anatase–rutile phase transformation on dielectric properties of sol–gel derived TiO_2 thin films. Jpn J Appl Phys 2005;44:6148. https://doi.org/10.1143/JJAP.44.6148.

[31] Ritcey A. Nanoparticles: properties and applications. Nano Online 2016. https://doi.org/10.1515/nano.0053.00004.

[32] Xiao Y, Wiesner MR. Nanoparticle Aggregation and Deposition in Porous Media. Engineered Nanoparticles and the Environment: Biophysicochemical Processes and Toxicity. John Wiley & Sons, Ltd; 2016; 224–44. https://doi.org/10.1002/9781119275855.ch12.

[33] Chen KL, Elimelech M. Aggregation and deposition kinetics of fullerene (C_{60}) nanoparticles. Langmuir 2006;22:10994–1001. https://doi.org/10.1021/la062072v.

[34] Zhang W. Nanoparticle aggregation: principles and modeling. Adv Exp Med Biol 2014;811:19–43. https://doi.org/10.1007/978-94-017-8739-0_2.

[35] Hiemenz PC, Rajagopalan R. Principles of colloid and surface chemistry, revised and expanded. 3 ed.New York: CRC Press; 1997.

[36] Wagner S, Gondikas A, Neubauer E, Hofmann T, von der Kammer F. Spot the difference: engineered and natural nanoparticles in the environment—release, behavior, and fate. Angew Chem Int Ed 2014;53:12398–419. https://doi.org/10.1002/anie.201405050.

[37] Buffle J, van Leeuwen HP. Environmental particles. Vol. 1. (IUPAC environmental analytical and physical chemistry series). Boca Raton, FL: CRC Press; 1992.

[38] ASTM E2865–12. Standard Guide for Measurement of Electrophoretic Mobility and Zeta Potential of Nanosized Biological Materials, 2012; 2018.

[39] Riddick TM, inc Z-M. Control of colloid stability through zeta potential: with a closing chapter on its relationship to cardiovascular disease. Zeta-Meter, inc.; 1968

[40] Kim AY, Berg JC. Fractal aggregation: scaling of fractal dimension with stability ratio. Langmuir 2000;16:2101–4. https://doi.org/10.1021/la990841n.

[41] Buffle J, Leppard GG. Characterization of aquatic colloids and macromolecules. 1. Structure and behavior of colloidal material. Environ Sci Technol 1995;29:2169–75. https://doi.org/10.1021/es00009a004.

[42] Elimelech M, Gregory J, Jia X, Willi ams RA. Chapter 3 - surface interaction potentials. In: Elimelech M, Gregory J, Jia X, Williams RA, editors. Particle Deposition & Aggregation. Woburn: Butterworth-Heinemann; 1995. p. 33–67. https://doi.org/10.1016/B978-075067024-1/50003-0.

[43] Israelachvili J. Intermolecular and surface forces. San Diego: Academic Press London; 1991.

[44] Levard C, Reinsch BC, Michel FM, Oumahi C, Lowry GV, Brown GE. Sulfidation processes of PVP-coated silver nanoparticles in aqueous solution: impact on dissolution rate. Environ Sci Technol 2011;45:5260–6. https://doi.org/10.1021/es2007758.

[45] Baalousha M, Manciulea A, Cumberland S, Kendall K, Lead JR. Aggregation and surface properties of iron oxide nanoparticles: influence of pH and natural organic matter. Environ Toxicol Chem 2008;27:1875–82. https://doi.org/10.1897/07-559.1.

[46] Lee K, Hwang Y, Cheong S, Kwon L, Kim S, Lee J. Performance evaluation of nanolubricants of fullerene nanoparticles in refrigeration mineral oil. Current Appl Phys 2009;9:e128–31. https://doi.org/10.1016/j.cap.2008.12.054.

[47] Xian-Ju W, Xin-Fang L. Influence of pH on Nanofluids' viscosity and thermal conductivity. Chinese Phys Lett 2009;26:056601. https://doi.org/10.1088/0256-307X/26/5/056601.

[48] Brant JA, Labille J, Robichaud CO, Wiesner M. Fullerol cluster formation in aqueous solutions: implications for environmental release. J Colloid Interface Sci 2007;314:281–8. https://doi.org/10.1016/j.jcis.2007.05.020.

[49] Liu J, Legros S, von der Kammer F, Hofmann T. Natural organic matter concentration and hydrochemistry influence aggregation kinetics of functionalized engineered nanoparticles. Environ Sci Technol 2013;47:4113–20. https://doi.org/10.1021/es302447g.

[50] Hu Z, Oskam G, Penn RL, Pesika N, Searson PC. The influence of anion on the coarsening kinetics of ZnO nanoparticles. J Phys Chem B 2003;107:3124–30. https://doi.org/10.1021/jp020580h.

[51] Ge J, Yin Y. Magnetically Tunable colloidal photonic structures in alkanol solutions. Adv Mater 2008;20:3485–91. https://doi.org/10.1002/adma.200800657.

[52] Fu R, Jin X, Liang J, Zheng W, Zhuang J, Yang W. Preparation of nearly monodispersed Fe_3O_4/SiO_2 composite particles from aggregates of Fe_3O_4 nanoparticles. J Mater Chem 2011;21:15352–6. https://doi.org/10.1039/C1JM11883H.

[53] Gesenhues U. Doping of TiO_2 pigments by Al^{3+}. Solid State Ion 1997;101–103:1171–80. https://doi.org/10.1016/S0167-2738(97)00443-8.

[54] Zhao Y, Wang M, Liu Y, Cui H. Redispersity/solubility of nanopowder in solvents. Recent Pat Nanotechnol 2014;8:18–30.

[55] Lee J-M, Kim D-W, Jun Y-D, Oh S-G. Process for synthesizing silver-silica particles and applications US7893104B2; 2011.

[56] Sato K, Kondo S, Tsukada M, Ishigaki T, Kamiya H. Influence of solid fraction on the optimum molecular weight of polymer dispersants in aqueous TiO_2 nanoparticle suspensions. J Am Ceram Soc 2007;90:3401–6. https://doi.org/10.1111/j.1551-2916.2007.01906.x.

[57] Tang F, Uchikoshi T, Ozawa K, Sakka Y. Effect of polyethylenimine on the dispersion and electrophoretic deposition of nano-sized titania aqueous suspensions. J Eur Ceram Soc 2006;26:1555–60. https://doi.org/10.1016/j.jeurceramsoc.2005.03.240.

[58] Kirby GH, Harris DJ, Li Q, Lewis JA. Poly(acrylic acid)–poly(ethylene oxide) comb polymer effects on $BaTiO_3$ nanoparticle suspension stability. J Am Ceram Soc 2004;87:181–6. https://doi.org/10.1111/j.1551-2916.2004.00181.x.

[59] Somosi Z, Pavlovic M, Pálinkó I, Szilágyi I. Effect of polyelectrolyte mono- and bilayer formation on the colloidal stability of layered double hydroxide nanoparticles. Nanomaterials (Basel) 2018;8. https://doi.org/10.3390/nano8120986.

[60] Katana B, Rouster P, Varga G, Muráth S, Glinel K, Jonas AM, et al. Self-assembly of protamine biomacromolecule on halloysite nanotubes for immobilization of superoxide dismutase enzyme. ACS Appl Bio Mater 2020;3:522–30. https://doi.org/10.1021/acsabm.9b00953.

[61] Sáringer S, Rouster P, Szilágyi I. Regulation of the stability of Titania Nanosheet dispersions with oppositely and like-charged polyelectrolytes. Langmuir 2019;35:4986–94. https://doi.org/10.1021/acs.langmuir.9b00242.

[62] V. Andre, H. Debus, J. Rieger (BASF AG), Patent WO 094156; 2005.

[63] Xiao Y, Chae S-R, Wiesner MR. Quantification of fullerene (C_{60}) in aqueous samples and use of C70 as surrogate standard. Chem Eng J 2011;170:555–61. https://doi.org/10.1016/j.cej.2011.03.073.

[64] Domingos RF, Tufenkji N, Wilkinson KJ. Aggregation of titanium dioxide nanoparticles: role of a fulvic acid. Environ Sci Technol 2009;43:1282–6. https://doi.org/10.1021/es8023594.

[65] Kamiya H, Iijima M. Surface modification and characterization for dispersion stability of inorganic nanometer-scaled particles in liquid media. Sci Technol Adv Mater 2010;11:044304. https://doi.org/10.1088/1468-6996/11/4/044304.

[66] Park J-W, Shumaker-Parry JS. Structural study of citrate layers on Gold nanoparticles: role of intermolecular interactions in stabilizing nanoparticles. J Am Chem Soc 2014;136:1907–21. https://doi.org/10.1021/ja4097384.

[67] Jana NR, Gearheart L, Murphy CJ. Seeding growth for size control of 5−40 nm diameter Gold nanoparticles. Langmuir 2001;17:6782–6. https://doi.org/10.1021/la0104323.

[68] Zhang S, Leem G, Srisombat L, Lee TR. Rationally designed ligands that inhibit the aggregation of large Gold nanoparticles in solution. J Am Chem Soc 2008;130:113–20. https://doi.org/10.1021/ja0724588.

[69] Iijima M, Kobayakawa M, Kamiya H. Tuning the stability of TiO_2 nanoparticles in various solvents by mixed silane alkoxides. J Colloid Interface Sci 2009;337:61–5. https://doi.org/10.1016/j.jcis.2009.05.007.

[70] Iijima M, Tajima S, Yamazaki M, Kamiya H. Redispersion property of TiO_2 nanoparticles modified with Oleyl-group. J Soc Powder Technol Jpn 2012;49:108–15. https://doi.org/10.4164/sptj.49.108.

[71] Iijima M, Takenouchi S, Lenggoro IW, Kamiya H. Effect of additive ratio of mixed silane alkoxides on reactivity with TiO_2 nanoparticle surface and their stability in organic solvents. Adv Powder Technol 2011;22:663–8. https://doi.org/10.1016/j.apt.2010.09.015.

[72] Niederberger M, Pinna N. Metal Oxide Nanoparticles in Organic Solvents: Synthesis, Formation, Assembly and Application. London: Springer-Verlag; 2009. https://doi.org/10.1007/978-1-84882-671-7.

[73] Debecker DP, Mutin PH. Non-hydrolytic sol–gel routes to heterogeneous catalysts. Chem Soc Rev 2012;41:3624–50. https://doi.org/10.1039/C2CS15330K.

[74] Deshmukh R, Niederberger M. Mechanistic aspects in the formation, growth and surface functionalization of metal oxide nanoparticles in organic solvents. Chem A Eur J 2017;23:8542–70. https://doi.org/10.1002/chem.201605957.

[75] Trentler TJ, Denler TE, Bertone JF, Agrawal A, Colvin VL. Synthesis of TiO_2 nanocrystals by nonhydrolytic solution-based reactions. J Am Chem Soc 1999;121:1613–4. https://doi.org/10.1021/ja983361b.

[76] Niederberger M, Bartl MH, Stucky GD. Benzyl alcohol and titanium TetrachlorideA versatile reaction system for the nonaqueous and low-temperature preparation of crystalline and luminescent Titania nanoparticles. Chem Mater 2002;14:4364–70. https://doi.org/10.1021/cm021203k.

[77] Garnweitner G, Grote C. In situ investigation of molecular kinetics and particle formation of water-dispersible titania nanocrystals. Phys Chem Chem Phys 2009;11:3767–74. https://doi.org/10.1039/B821973G.

[78] Garnweitner G, Ghareeb HO, Grote C. Small-molecule in situ stabilization of TiO_2 nanoparticles for the facile preparation of stable colloidal dispersions. Colloids Surf A Physicochem Eng Asp 2010;372:41–7. https://doi.org/10.1016/j.colsurfa.2010.09.024.

[79] Misra TK, Liu C-Y. Synthesis, isolation, and redispersion of resorcinarene-capped anatase TiO2nanoparticles in nonaqueous solvents. Journal of Colloid and Interface Science 2007;310:178–83. https://doi.org/10.1016/j.jcis.2007.01.094.

[80] Aboulaich A, Boury B, Mutin PH. Reactive and organosoluble anatase nanoparticles by a surfactant-free nonhydrolytic synthesis. Chem Mater 2010;22:4519–21. https://doi.org/10.1021/cm101191a.

[81] Aboulaich A, Lorret O, Boury B, Mutin PH. Surfactant-free Organo-soluble silica−Titania and silica nanoparticles. Chem Mater 2009;21:2577–9. https://doi.org/10.1021/cm900291p.

[82] Aboulaich A, Boury B, Mutin PH. Reactive and Organosoluble SnO_2 nanoparticles by a surfactant-free non-hydrolytic sol–gel route. Eur J Inorganic Chem 2011;2011:3644–9. https://doi.org/10.1002/ejic.201100391.

[83] Dalmaschio CJ, Leite ER. Detachment induced by Rayleigh-instability in metal oxide Nanorods: insights from TiO_2. Cryst Growth Des 2012;12:3668–74. https://doi.org/10.1021/cg300473u.

[84] Fominykh K, Feckl JM, Sicklinger J, Döblinger M, Böcklein S, Ziegler J, et al. Water splitting: ultrasmall dispersible crystalline nickel oxide nanoparticles as high-performance catalysts for electrochemical water splitting. Adv Funct Mater 2014;24:3105. https://doi.org/10.1002/adfm.201470134.

[85] Hu Y, Zhou S, Wu L. Surface mechanical properties of transparent poly(methyl methacrylate)/zirconia nanocomposites prepared by in situ bulk polymerization. Polymer 2009;50:3609–16. https://doi.org/10.1016/j.polymer.2009.03.028.

[86] Zhou S, Wu L. Phase separation and properties of UV-curable polyurethane/zirconia nanocomposite coatings. Macromol Chem Phys 2008;209:1170–81. https://doi.org/10.1002/macp.200800090.

[87] De Roo J, Van den Broeck F, De Keukeleere K, Martins JC, Van Driessche I, Hens Z. Unravelling the surface chemistry of metal oxide nanocrystals, the role of acids and bases. J Am Chem Soc 2014;136:9650–7. https://doi.org/10.1021/ja5032979.

[88] da Silva RO, Conti TG, de Moura AF, Stroppa DG, Freitas LCG, Ribeiro C, et al. Antimony-doped tin oxide nanocrystals: synthesis and solubility behavior in organic solvents. ChemPhysChem 2009;10:841–6. https://doi.org/10.1002/cphc.200800764.

[89] De Roo J, Coucke S, Rijckaert H, De Keukeleere K, Sinnaeve D, Hens Z, et al. Amino acid-based stabilization of oxide nanocrystals in polar media: from insight in ligand exchange to solution 1H NMR probing of short-chained adsorbates. Langmuir 2016;32:1962–70. https://doi.org/10.1021/acs.langmuir.5b04611.

[90] Rutnakornpituk M, Meerod S, Boontha B, Wichai U. Magnetic core-bilayer shell nanoparticle: a novel vehicle for entrapmentof poorly water-soluble drugs. Polymer 2009;50:3508–15. https://doi.org/10.1016/j.polymer.2009.06.015.

[91] Cai W, Wan J. Facile synthesis of superparamagnetic magnetite nanoparticles in liquid polyols. J Colloid Interface Sci 2007;305:366–70. https://doi.org/10.1016/j.jcis.2006.10.023.

[92] Guo JJ, Lewis JA. Aggregation effects on the compressive flow properties and drying behavior of colloidal silica suspensions. J Am Ceram Soc 1999;82:2345–58. https://doi.org/10.1111/j.1151-2916.1999.tb02090.x.

[93] Hunter RJ. Foundations of colloid science. Clarendon Press; 1989.

[94] Chiu RC, Garino TJ, Cima MJ. Drying of granular ceramic films: I, effect of processing variables on cracking behavior. J Am Ceram Soc 1993;76:2257–64. https://doi.org/10.1111/j.1151-2916.1993.tb07762.x.

[95] Chiu RC, Cima MJ. Drying of granular ceramic films: II, drying stress and saturation uniformity. J Am Ceram Soc 1993;76:2769–77. https://doi.org/10.1111/j.1151-2916.1993.tb04014.x.

[96] Vertanessian A, Allen A, Mayo MJ. Agglomerate formation during drying. J Materials Res 2003;18:495–506. https://doi.org/10.1557/JMR.2003.0063.

[97] Suryawanshi C, Pakdel P, Schaefer D. Effect of drying on the structure and dispersion of precipitated silica. J Appl Cryst 2003;36. https://doi.org/10.1107/S0021889803001729.

[98] Wang W-N, Lenggoro IW, Okuyama K. Dispersion and aggregation of nanoparticles derived from colloidal droplets under low-pressure conditions. J Colloid Interface Sci 2005;288:423–31. https://doi.org/10.1016/j.jcis.2005.03.010.

[99] Iskandar F, Lenggoro IW, Xia B, Okuyama K. Functional nanostructured silica powders derived from colloidal suspensions by sol spraying. J Nanopart Res 2001;3:263–70. https://doi.org/10.1023/A:1017592817667.

[100] Zellmer S, Lindenau M, Michel S, Garnweitner G, Schilde C. Influence of surface modification on structure formation and micromechanical properties of spray-dried silica aggregates. J Colloid Interface Sci 2016;464:183–90. https://doi.org/10.1016/j.jcis.2015.11.028.

[101] Abdelwahed W, Degobert G, Stainmesse S, Fessi H. Freeze-drying of nanoparticles: formulation, process and storage considerations. Adv Drug Deliv Rev 2006;58:1688–713. https://doi.org/10.1016/j.addr.2006.09.017.

[102] Wolkers WF, Oldenhof H, editors. Cryopreservation and freeze-drying protocols. 3rd ed. New York: Springer-Verlag; 2015. https://doi.org/10.1007/978-1-4939-2193-5.

[103] Vishali DA, Monisha J, Sivakamasundari SK, Moses JA, Anandharamakrishnan C. Spray freeze drying: emerging applications in drug delivery. J Control Release 2019;300:93–101. https://doi.org/10.1016/j.jconrel.2019.02.044.

[104] Amstad E, Zurcher S, Mashaghi A, Wong JY, Textor M, Reimhult E. Surface functionalization of single superparamagnetic Iron oxide nanoparticles for targeted magnetic resonance imaging. Small 2009;5:1334–42. https://doi.org/10.1002/smll.200801328.

[105] Sameti M, Bohr G, Ravi Kumar MNV, Kneuer C, Bakowsky U, Nacken M, et al. Stabilisation by freeze-drying of cationically modified silica nanoparticles for gene delivery. Int J Pharm 2003;266:51–60. https://doi.org/10.1016/s0378-5173(03)00380-6.

[106] Siedl N, Baumann SO, Elser MJ, Diwald O. Particle networks from powder mixtures: generation of TiO_2–SnO_2 heterojunctions via surface charge-induced Heteroaggregation. J Phys Chem C Nanomater Interfaces 2012;116:22967–73. https://doi.org/10.1021/jp307737s.

[107] Liepa T. Nano-measurements: Complete list of protocols. NIST; 2015. https://www.nist.gov/mml/nano-measurements-complete-list-protocols, Accessed date: 5 November 2019.

[108] Burrows ND, Kesselman E, Sabyrov K, Stemig A, Talmon Y, Penn RL. Crystalline nanoparticle aggregation in non-aqueous solvents. CrystEngComm 2014;16:1472–81. https://doi.org/10.1039/c3ce41584h.

[109] Siddiqui SW, Unwin PJ, Xu Z, Kresta SM. The effect of stabilizer addition and sonication on nanoparticle agglomeration in a confined impinging jet reactor. Colloids Surf A Physicochem Eng Asp 2009;350:38–50. https://doi.org/10.1016/j.colsurfa.2009.08.031.

[110] Mandzy N, Grulke E, Druffel T. Breakage of TiO_2 agglomerates in electrostatically stabilized aqueous dispersions. Powder Technol 2005;160:121–6. https://doi.org/10.1016/j.powtec.2005.08.020.

[111] Sato K, Li J-G, Kamiya H, Ishigaki T. Ultrasonic dispersion of TiO_2 nanoparticles in aqueous suspension. J Am Ceram Soc 2008;91:2481–7. https://doi.org/10.1111/j.1551-2916.2008.02493.x.

[112] Qiu G, Wang Q, Nie M. Polypyrrole-Fe_3O_4 magnetic nanocomposite prepared by ultrasonic irradiation. Macromol Mater Eng 2006;291:68–74. https://doi.org/10.1002/mame.200500285.

[113] Schaefer DW, Kohls D, Feinblum E. Morphology of highly dispersing precipitated silica: impact of drying and sonication. J Inorg Organomet Polym 2012;22:617–23. https://doi.org/10.1007/s10904-011-9643-y.

[114] Zhang Y, Chen Y, Westerhoff P, Hristovski K, Crittenden JC. Stability of commercial metal oxide nanoparticles in water. Water Res 2008;42:2204–12. https://doi.org/10.1016/j.watres.2007.11.036.

[115] Iijima M. Surface modification techniques toward controlling the dispersion stability and particle-assembled structures of slurries. J Cerma Soc Jpn 2017;125:603–7. https://doi.org/10.2109/jcersj2.17093.

[116] Degand S, Lamblin G, Dupont-Gillain CC. Colloidal lithography using silica particles: improved particle distribution and tunable wetting properties. J Colloid Interface Sci 2013;392:219–25. https://doi.org/10.1016/j.jcis.2012.10.011.

[117] Hanarp P, Sutherland DS, Gold J, Kasemo B. Control of nanoparticle film structure for colloidal lithography. Colloids Surf A Physicochem Eng Asp 2003;214:23–36. https://doi.org/10.1016/S0927-7757(02)00367-9.

[118] Nonckreman CJ, Fleith S, Rouxhet PG, Dupont-Gillain CC. Competitive adsorption of fibrinogen and albumin and blood platelet adhesion on surfaces modified with nanoparticles and/or PEO. Colloids Surf B Biointerfaces 2010;77:139–49. https://doi.org/10.1016/j.colsurfb.2010.01.014.

[119] Drelich JW. Contact angles: from past mistakes to new developments through liquid-solid adhesion measurements. Adv Colloid Interface Sci 2019;267:1–14. https://doi.org/10.1016/j.cis.2019.02.002.

[120] Qian J, Bhawalkar SP, Xu Y, Jia L. Novel use of polymer brushes in colloidal lithography to overcome lateral capillary force. ACS Appl Mater Interfaces 2010;2:3111–8. https://doi.org/10.1021/am100608k.

[121] Thill A, Spalla O. Aggregation due to capillary forces during drying of particle submonolayers. Colloids Surf A Physicochem Eng Asp 2003;217:143–51. https://doi.org/10.1016/S0927-7757(02)00569-1.

[122] Tohver V, Smay JE, Braem A, Braun PV, Lewis JA. Nanoparticle halos: a new colloid stabilization mechanism. PNAS 2001;98:8950–4. https://doi.org/10.1073/pnas.151063098.

[123] Viota JL, González-Caballero F, Durán JDG, Delgado AV. Study of the colloidal stability of concentrated bimodal magnetic fluids. J Colloid Interface Sci 2007;309:135–9. https://doi.org/10.1016/j.jcis.2007.01.066.

[124] Morisada S, Kojima S, Sumi T, Kawakita H, Ohto K. Fabrication of non-close-packed colloidal monolayers by convective self-assembly using cationic polyelectrolyte-grafted silica particles. Colloid Polym Sci 2015;293:2985–93. https://doi.org/10.1007/s00396-015-3706-5.

[125] Jang HD, Cho K, Kim B-G. Fabrication method of $CaCO_3$ nanoparticles using beads milling US8048932B2 ; 2011.

[126] Niederberger M, Garnweitner G, Krumeich F, Nesper R, Cölfen H, Antonietti M. Tailoring the surface and solubility properties of Nanocrystalline Titania by a non-aqueous in situ functionalization process. Chem Mater 2004;16:1202–8. https://doi.org/10.1021/cm031108r.

[127] Nakayama N, Hayashi T. Preparation and characterization of TiO_2 and polymer nanocomposite films with high refractive index. J Appl Polym Sci 2007;105:3662–72. https://doi.org/10.1002/app.26451.

[128] Mori K, Nakamura M, Tanaka M. Titanium oxide colloidal sol and process for the preparation thereof US6420437B1 ; 2002.

[129] Tasbihi M, Štangar UL, Černigoj U, Kogej K. Low-temperature synthesis and characterization of anatase TiO_2 powders from inorganic precursors. Photochem Photobiol Sci 2009;8:719–25. https://doi.org/10.1039/B817472E.

[130] Kho K, Hadinoto K. Aqueous re-dispersibility characterization of spray-dried hollow spherical silica nano-aggregates. Powder Technol 2010;198:354–63. https://doi.org/10.1016/j.powtec.2009.11.031.

[131] Silvestri B, Costantini A, Speranza V, Luciani G, Branda F, Russo P. Agglomeration-free silica NPs in dry storage for PBT nanocomposite. J Sol-Gel Sci Technol 2016;78:531–8. https://doi.org/10.1007/s10971-016-3985-4.

[132] Jeevanandam J, Barhoum A, Chan YS, Dufresne A, Danquah MK. Review on nanoparticles and nanostructured materials: history, sources, toxicity and regulations. Beilstein J Nanotechnol 2018;9:1050–74. https://doi.org/10.3762/bjnano.9.98.

[133] Wohlleben W, Punckt C, Aghassi-Hagmann J, Siebers F, Menzel F, Esken D, et al. Nanoenabled Products: Categories, Manufacture, and Applications. Metrology and Standardization of Nanotechnology. John Wiley & Sons, Ltd; 2017; 409–64. https://doi.org/10.1002/9783527800308.ch25.

[134] Becheri A, Dürr M, Lo Nostro P, Baglioni P. Synthesis and characterization of zinc oxide nanoparticles: application to textiles as UV-absorbers. J Nanopart Res 2008; 10:679–89. https://doi.org/10.1007/s11051-007-9318-3.

[135] Kelly FM, Johnston JH. Colored and functional silver nanoparticle-wool fiber composites. ACS Appl Mater Interfaces 2011;3:1083–92. https://doi.org/10.1021/am101224v.

[136] Kim JB, Kim JY, Yoon TH. Determination of silver nanoparticle species released from textiles into artificial sweat and laundry wash for a risk assessment. Hum Ecol Risk Assess Int J 2017;23:741–50. https://doi.org/10.1080/10807039.2016.1277417.

[137] Scott K, Pomar-Portillo V, Vázquez-Campos S. Nanomaterials in Textiles. Metrology and Standardization of Nanotechnology. John Wiley & Sons, Ltd; 2017; 559–72. https://doi.org/10.1002/9783527800308.ch31.

[138] Alongi J, Ciobanu M, Malucelli G. Thermal stability, flame retardancy and mechanical properties of cotton fabrics treated with inorganic coatings synthesized through sol–gel processes. Carbohydr Polym 2012;87:2093–9. https://doi.org/10.1016/j.carbpol.2011.10.032.

[139] Lee S. Developing UV-protective textiles based on electrospun zinc oxide nanocomposite fibers. Fibers Polym 2009;10:295–301. https://doi.org/10.1007/s12221-009-0295-2.

[140] Sun J, Ma D, Zhang H, Liu X, Han X, Bao X, et al. Toward monodispersed silver nanoparticles with unusual thermal stability. J Am Chem Soc 2006;128:15756–64. https://doi.org/10.1021/ja064884j.

[141] Joo SH, Park JY, Tsung C-K, Yamada Y, Yang P, Somorjai GA. Thermally stable Pt/mesoporous silica core–shell nanocatalysts for high-temperature reactions. Nat Mater 2009;8:126–31. https://doi.org/10.1038/nmat2329.

[142] Phenrat T, Kim H-J, Fagerlund F, Illangasekare T, Tilton RD, Lowry GV. Particle size distribution, concentration, and magnetic attraction affect transport of polymer-modified Fe0 nanoparticles in sand columns. Environ Sci Technol 2009;43:5079–85. https://doi.org/10.1021/es900171v.

[143] Lázár I, Szabó HJ. Prevention of the aggregation of nanoparticles during the synthesis of Nanogold-containing silica aerogels. Gels 2018;4. https://doi.org/10.3390/gels4020055.

[144] Thaptong P, Sae-oui P, Sirisinha C. Influences of styrene butadiene rubber and silica types on performance of passenger car radial tire tread. Rubber Chem Technol 2017;90:699–713. https://doi.org/10.5254/rct.17.83724.

[145] Nemati A, Goharian P, Shabanian M, Afshar A. Effects of nucleation agent particle size on properties, crystallisation and microstructure of glass-ceramics in TiO_2-ZrO_2-Li_2O-CaO- Al_2O_3-SiO_2 system. Adv Appl Ceramics 2010;109:318–23. https://doi.org/10.1179/174367609X422063.

[146] DiDomizio R, Huang S, Dial L, Ilavsky J, Larsen M. An assessment of milling time on the structure and properties of a nanostructured ferritic alloy (NFA). Metallurg Materials Trans A 2014;45. https://doi.org/10.1007/s11661-014-2521-9.

[147] Napper DH. Steric stabilization. J Colloid Interface Sci 1977;58:390–407. https://doi.org/10.1016/0021-9797(77)90150-3.

[148] Zimmermann I, Eber M, Meyer K. Nanomaterials as flow regulators in dry powders. Zeitschrift Für Physikalische Chemie 2004;218:51–102. https://doi.org/10.1524/zpch.218.1.51.25388.

[149] Kharisov BI, Dias HVR, Kharissova OV, Vázquez A, Peña Y, Gómez I. Solubilization, dispersion and stabilization of magnetic nanoparticles in water and non-aqueous solvents: recent trends. RSC Adv 2014;4:45354–81. https://doi.org/10.1039/C4RA06902A.

[150] Wu W, Jiang CZ, Roy VAL. Designed synthesis and surface engineering strategies of magnetic iron oxide nanoparticles for biomedical applications. Nanoscale 2016;8:19421–74. https://doi.org/10.1039/C6NR07542H.

[151] Castelo-Grande T, Augusto PA, Estevez A, Barbosa D, Rodriguez J, et al. Magnetically stabilized and fluidized beds in science and technology: A review. In: Vafai K, editor. Handbook of porous media. 3rd ed. Hoboken, NJ: CRC Press; 2015. p. 113–56. https://doi.org/10.1201/b18614.

[152] Doganay S, Alsangur R, Turgut A. Effect of external magnetic field on thermal conductivity and viscosity of magnetic nanofluids: a review. Mater Res Express 2019;6:112003. https://doi.org/10.1088/2053-1591/ab44e9.

[153] Korpany KV, Habib F, Murugesu M, Blum AS. Stable water-soluble iron oxide nanoparticles using Tiron. Mater Chem Phys 2013;138:29–37. https://doi.org/10.1016/j.matchemphys.2012.10.015.

[154] Liang Z, Wu X, Xie Y, Liu S. A facile approach to fabricate water-soluble au-Fe_3O_4 nanoparticle for liver Cancer cells imaging. Chin J Chem 2012;30:1387–92. https://doi.org/10.1002/cjoc.201100692.

[155] Hui C, Shen C, Yang T, Bao L, Tian J, Ding H, et al. Large-scale Fe_3O_4 nanoparticles soluble in water synthesized by a facile method. J Phys Chem C 2008;112:11336–9. https://doi.org/10.1021/jp801632p.

[156] Gul S, Kausar A, Muhammad B, Jabeen S. Research Progress on properties and applications of polymer/clay nanocomposite. Polym-Plast Technol Eng 2016;55:684–703. https://doi.org/10.1080/03602559.2015.1098699.

[157] Patel HA, Somani RS, Bajaj HC, Jasra RV. Nanoclays for polymer nanocomposites, paints, inks, greases and cosmetics formulations, drug delivery vehicle and waste water treatment. Bull Mater Sci 2006;29:133–45. https://doi.org/10.1007/BF02704606.

[158] Lagaron JM, Busolo M. Antimicrobial plastics based on metal-containing Nanolayered clays. Antimicrobial Polymers 2011:317–26. https://doi.org/10.1002/9781118150887.ch12.

[159] Di Sarli V, Landi G, Lisi L, Di Benedetto A. Ceria-coated diesel particulate filters for continuous regeneration. AIChE J 2017;63:3442–9. https://doi.org/10.1002/aic.15688.

[160] Balamurugan S, Sajith V. Experimental investigation on the stability and abrasive action of cerium oxide nanoparticles dispersed diesel. Energy 2017;131:113–24. https://doi.org/10.1016/j.energy.2017.05.032.

[161] Ghadimi A, Saidur R, Metselaar HSC. A review of nanofluid stability properties and characterization in stationary conditions. Int J Heat Mass Transfer 2011;54:4051–68. https://doi.org/10.1016/j.ijheatmasstransfer.2011.04.014.

[162] Chung SJ, Leonard JP, Nettleship I, Lee JK, Soong Y, Martello DV, et al. Characterization of ZnO nanoparticle suspension in water: effectiveness of ultrasonic dispersion. Powder Technol 2009;194:75–80. https://doi.org/10.1016/j.powtec.2009.03.025.

[163] Chang H, Jwo CS, Fan PS, Pai SH. Process optimization and material properties for nanofluid manufacturing. Int J Adv Manuf Technol 2007;34:300–6. https://doi.org/10.1007/s00170-006-0597-0.

[164] Mahshid S, Askari M, Ghamsari MS. Synthesis of TiO_2 nanoparticles by hydrolysis and peptization of titanium isopropoxide solution. J Mater Process Technol 2007;189:296–300. https://doi.org/10.1016/j.jmatprotec.2007.01.040.

[165] Seo J, Chung H, Kim M, Lee J, Choi I, Cheon J. Development of water-soluble single-crystalline TiO_2 nanoparticles for photocatalytic cancer-cell treatment. Small 2007;3:850–3. https://doi.org/10.1002/smll.200600488.

[166] Bachinger A, Kickelbick G. Pickering emulsions stabilized by anatase nanoparticles. Monatsh Chem 2010;141:685–90. https://doi.org/10.1007/s00706-010-0273-9.

[167] Cao H, Zhang X, Ding B, Wang L, Lu N. Synergistic action of TiO_2 particles and surfactants on the foamability and stabilization of aqueous foams. RSC Adv 2017;7:44972–8. https://doi.org/10.1039/C7RA08394G.